NASA Technical Memorandum 78768

Improvements to the FATOLA Computer Program Including Nosewheel Steering

Supplemental Instruction Manual

Huey D. Carden and John R. McGehee

DECEMBER 1978

NASA

NASA Technical Memorandum 78768

Improvements to the FATOLA Computer Program Including Nosewheel Steering

Supplemental Instruction Manual

Huey D. Carden and John R. McGehee
Langley Research Center
Hampton, Virginia

National Aeronautics
and Space Administration

**Scientific and Technical
Information Office**

1978

SUMMARY

Modifications to improve the analytical simulation capabilities of a multi-degree-of-freedom flexible aircraft take-off and landing analysis (FATOLA) computer program are discussed, and supplemental instructions are included in an appendix for users of the FATOLA computer program. Sample results presented to illustrate the capabilities of an added nosewheel steering option indicate consistent behavior of the airplane tracking, attitude, motions, and loads for the landing cases and steering situations that were investigated.

INTRODUCTION

Experimental and analytical research is being conducted by the Langley Research Center to acquire accurate predictions of ground-induced loads and vibrations of airplanes and to develop active control landing-gear systems (ref. 1) which limit the loads transmitted through the gear to the airframe. To obtain improved analytical prediction of the airframe structural response, the multi-degree-of-freedom take-off and landing analysis (TOLA) computer program of references 2 to 5 was modified (refs. 6 and 7) to include effects of airframe flexibility on the loads and motions. The modified program called FATOLA (flexible aircraft take-off and landing analysis), which was validated in reference 8 with flight landing data, provides a comprehensive simulation of the airplane take-off and landing dynamics.

The purpose of this paper is to describe subsequent additional modifications made to the FATOLA program to improve its simulation capabilities and to present an appendix of supplemental instructions for users of the FATOLA computer program. Sample analytical results which illustrate the capabilities of the added nosewheel steering option are also presented.

Although the data are given in both SI and U.S. Customary Units, the measurements and calculations were made in U.S. Customary Units.

FATOLA COMPUTER PROGRAM

Capabilities

The general capabilities of the FATOLA computer program are illustrated in figure 1. FATOLA is a modified version of the original rigid-body computer program TOLA (take-off and landing analysis) of references 2 to 5. NASA Langley Research Center obtained the original program and added a flexible-body option (refs. 6 and 7) to generate the FATOLA program which has a core requirement of approximately 115 000 octal words on a Control Data 6600 digital computer. As indicated in figure 1, FATOLA provides a comprehensive simulation of the airplane take-off and landing dynamics. The program can represent an airplane either as a rigid body with six degrees of freedom or as a flexible body with

multiple degrees of freedom. The airframe flexibility is represented by the superposition of from 1 to 20 free vibration modes on the rigid-body motions. The analysis has maneuver logic and autopilots programmed to control the airplane during glide slope, flare, landing, and take-off. The program is modular so that performance of the airplane in flight and during landing and ground maneuvers can be studied separately or in combination.

Data which describe runway roughness, vehicle geometry, flexibility and aerodynamic characteristics, landing gear, propulsion, and initial conditions such as attitude, attitude change rates, and velocities are input to the program. A time integration of the equations of motion is performed to output comprehensive information on the airframe, state-of-maneuver logic, autopilots, control response, and airplane loads from impact, runway roll-out, and ground operations for both the rigid-body and flexible-body options. Flexible-body and total (elastic plus rigid-body) displacements, velocities, and accelerations are also output in the flexible-body option for up to 20 points on the airplane. Complete details of the program formulation and capabilities are given in references 2 to 8.

Subsequent to the publication of references 6 and 7, modifications (see ref. 8) were made at Langley Research Center to improve the analytical simulation capabilities of the FATOLA computer program. These changes and additional program modifications to accommodate new input data consistent with the original FATOLA data deck are discussed in the following sections. Supplemental user instructions for the modifications are presented in appendix A and details of their incorporation into FATOLA are given in appendix B.

Modifications

Strut axial friction.- In the original program the force in the struts attributed to axial friction was included as the component of the resultant ground force normal to the strut multiplied by a coefficient of friction applied to oppose strut motion. This formulation (ref. 9) is incomplete because the normal bearing forces depend on the moments applied to the struts. To improve the axial friction formulation, a new friction-force equation was introduced to include the moment effects. In addition, the smoothing technique discussed in reference 10 was included to prevent a sudden change in magnitude and direction of the friction force at the time the strut velocity changes sign, and a modification was made to allow the friction force to act before strut motion occurs as would be the case in the actual strut.

Strut air pressure equations.- A modification was made to the FATOLA program in the equations for the air pressures in the upper and lower air chambers of the strut. In the pressure equations the relationship

$$pV^{\gamma} = \text{Constant}$$

was originally programmed with the ratio of specific heats γ equal to 1.0 (where V is strut air volume and p is gage pressure). Changes were made to use absolute pressure in the pV relationship and to allow γ to take on values other than 1.0.

Strut vapor pressure.- Since hydraulic pressure could drop to vapor pressure in the strut during extension for gears with snubber valves, appropriate tests were added to determine when vapor pressure exists and a shock-strut force equation was added for this condition.

Structural damping.- In references 6 and 7 the dynamic motion of the airplane body is described by the normal mode method, in which the body flexibility is represented by free vibration modes with no structural damping. In the flexible-body option an equivalent viscous damping formulation (ref. 11) was added to prevent possible analytical divergence in the flexible-body response.

Roll and yaw autopilots.- Originally, the FATOLA program logic in the roll autopilot placed the aileron deflection to a neutral setting at the time of landing impact. For an asymmetric landing of an airplane, the pilot would likely introduce aileron and rudder deflections along with pitch control in the impact and roll-out phases of the landing. Changes in the roll autopilot logic were therefore made to permit the simulation of variations in roll-control deflections and rolling moments throughout the landing. Similar changes were also included in the yaw autopilot to permit simulation of variations in rudder-control deflections and yawing moments.

Nosewheel steering.- An option for nosewheel steering was added to enhance control of the airplane simulation during take-off and landing. This required the incorporation of nosewheel steering and main-wheel ground plane forces into the program and the addition of a nosewheel steering autopilot.

Empirical equations from reference 12 which express tire forces as a function of the tire vertical load, yaw angle, and coefficient of friction were included in FATOLA. However, the modified program does not include the effects of self-aligning torque or pneumatic caster.

The nosewheel steering autopilot may be operated in a variety of ways. It can be configured to maintain a preselected airplane heading with respect to the runway (airplane yaw angle) or to control the aircraft lateral drift during the landing or take-off roll. The autopilot can maintain a preselected constant nose steering angle relative to the aircraft or may be programmed to follow a given steering input time history. A variation of this last option permits automatic coupling of the rudder and nosewheel. The coupling is linear and based upon the ratio of the limits of the nosewheel steering angle to the rudder deflection. No lag is included in the coupled mode.

New input/output data.- The above FATOLA program modifications require new input data on strut bearing spacing, distance of hub to lower bearing, ratio of specific heats, modal damping values, nosewheel steering inputs, and appropriate indicators. The FATOLA program was altered to include these new input data as part of the normal FATOLA data input deck.

Appropriate changes in the FATOLA program and its plotting program PLTDAT were also made to allow several new variables associated with the steering option to be printed as part of the normal FATOLA data output and stored on tape for subsequent plotting. The data modifications, as well as the program modifications discussed above, are identified in the appendixes. It should be

noted that all COMMON,READ,WRITE, and FORMAT statements, which were temporarily included in the program due to changes given in reference 8, have been deleted as part of the current changes.

FATOLA ANALYTICAL RESULTS

General

To illustrate the effects of the nosewheel steering option in FATOLA, sample analytical results are presented for the landing impact and roll-out of a supersonic cruise airplane shown in figure 2. For each case the touchdown parameters were: sink rate, 0.67 m/sec (2.2 ft/sec); ground speed, 97.9 m/sec (321 ft/sec); pitch angle, 7.2°; initial pitch rate, -0.4 deg/sec (nose over); angle of attack, 7.65°; roll rate, 0.0 deg/sec. Idle thrust was simulated for two jet engines and a drag parachute was deployed 10 sec after touchdown. The dry landing surface was runway 22 at Edwards Air Force Base, California, which had the roughness profile described in reference 8. For the cases involving nosewheel steering, it was engaged at nose-gear contact. The steering-angle limits were set at ±25°. The steering rate was 10 deg/sec and the feedback constant was 20 sec.

Touchdown conditions were selected to illustrate several, but not all, features of the nosewheel steering option. The following sections will compare the reactions of a simulated airplane under rudder control only with those of an airplane under coupled rudder-nosewheel steering. Consistent behavior of the airplane tracking, attitude, motions, and loads will demonstrate the capability of the nosewheel steering option to control a simulated airplane during a crosswind landing. The effect that main-gear tire side forces have on the response characteristics predicted by FATOLA will be described.

Comparison of Aircraft Controlled by Rudder Only and by Coupled Rudder-Nosewheel Steering

Figure 3 presents the input rudder-control deflections, nosewheel steering angles, nosewheel yaw angles, pitch attitude, pitch rates, nosewheel steering forces, airplane c.g. position on the runway, strut strokes, and axial strut forces for touchdowns of the supersonic cruise airplane 16.8 m (55 ft) to the right of the runway center line (no crosswind) with control by rudder deflections only, and with rudder control automatically coupled to the nosewheel. The control inputs were arbitrarily chosen to exercise the program logic and to verify the equations associated with the coupled rudder-nosewheel steering. No attempt was made to keep the simulated airplane within the confines of the runway, and consequently, the airplane departed the left side of the runway approximately 7.8 and 10 sec after touchdown for the two landings of figure 3.

Rudder deflection.- The input rudder deflections, which are identical for the two landings, are presented in figure 3(a). Nose-gear touchdown at approximately 2.7 sec and drag parachute deployment at 10 sec are indicated on the figure along with the times when the airplane left the runway.

Nosewheel steering angle.- The analytical variations of the nosewheel steering angle for the two landings of the simulated airplane are presented in figure 3(b). As programmed the nosewheel steering angle for rudder control only is zero throughout the touchdown and roll-out. For the landing with coupled rudder-nosewheel steering, the variations of the nosewheel steering angle are similar to the rudder deflections but are of opposite sign and differ in magnitude because of the steering ratio (ratio of the limits of nosewheel angle to rudder deflection) used in the steering autopilot.

Nosewheel yaw angle.- Figure 3(c) presents the variations of the nosewheel yaw angle, measured between the axle velocity vector and the wheel plane, for the two landing cases. The nosewheel yaw angle for rudder control only reached about -3.5° at approximately 7 sec and was still slightly negative at 10 sec, the time the airplane reached the left edge of the runway. For the coupled rudder-nosewheel control, the yaw-angle variations are similar to the steering-angle variations but differ in magnitude because of variations in airplane yaw angle.

Pitch attitude.- The pitch-attitude time histories for the two landing conditions are shown in figure 3(d). After approximately 5 sec, rudder control only caused few changes in pitch and the airplane settled into its normal 3-point attitude. During the same time span, coupled rudder-nosewheel steering continually altered the load distribution among the three landing gears which resulted in variations in the airplane pitch attitude.

Pitch rate.- The corresponding pitch rates for the two landing cases are presented in figure 3(e). For both landing conditions, the pitch rate was approximately -0.16 rad/sec (nose over) at the time of nose-gear touchdown, and subsequently the pitch rate went through $1\frac{1}{2}$ cycles of oscillation. After approximately 5 sec the pitch rate settled to small variations about zero for rudder control only but exhibited a more dynamic characteristic for coupled rudder-nosewheel steering.

Nosewheel steering force.- Time histories of nosewheel steering forces are presented in figure 3(f) for the two landing conditions. For rudder control only the nosewheel generated a maximum steering force of approximately 6.73 kN (1513 lbf). As expected for coupled rudder-nosewheel steering, the nosewheel generated larger steering forces (approximately 4 times greater) than the fixed nose gear. In both cases the nosewheel steering force, which is a function of the tire yaw angle and the vertical load, reflects the oscillatory effects of airplane pitching motions. The largest oscillations are, of course, evident in the coupled rudder-nosewheel landing for which more dynamic pitching motions occurred.

Airplane c.g. runway position.- Figure 3(g) presents the airplane c.g. cross range (lateral) runway position as a function of down range (longitudinal) runway position for both landing cases. Time along the trajectories is also indicated. Touchdown was 16.8 m (55 ft) to the right of the runway center line. For the landing with rudder control only, the arbitrary rudder deflection initiated a left yawing motion which eventually led the airplane to the left

edge of the runway approximately 0.90 km (3000 ft) after touchdown. For the landing with coupled rudder-nosewheel steering the airplane left the runway approximately 0.73 km (2400 ft) down range. These results clearly illustrate the increased effectiveness of the coupled rudder-nosewheel steering.

Strut stroke.- Figures 3(h) to 3(j) present the strut strokes of the right main, left main, and nose gears for the two landing cases being considered. Zero stroke is for a fully extended gear. In both cases the behavior of the strut stroke is indicative of the basic motions of the airplane. For example, as the airplane c.g. traversed the path shown in figure 3(g) the airplane yawed left and rolled right; consequently the right-main-gear stroke increased and the left-main-gear stroke decreased as shown in figures 3(h) and 3(i), respectively. Under the influence of coupled rudder-nosewheel steering the airplane yaw and roll motions were large enough to cause the left main gear to lose contact with the runway for approximately 2 sec as shown in figure 3(i).

The nose-gear strut strokes presented in figure 3(j) for both landing cases show differences which are related to the directional control inputs. After the initial nose-gear stroke pulse and subsequent loss of contact with the runway at approximately 3.5 sec, the second stroke pulse of the nose gear for the landing with rudder control only was higher than that for coupled rudder-nosewheel steering. The reduced stroke of the coupled-steering case is attributed in part to higher binding forces in the gear resulting from greater nosewheel yaw angles. (See figs. 3(c) and 3(f).)

Axial strut force.- Figures 3(k) to 3(m) are the axial strut forces which developed during the two landing cases. Since the axial strut force in the landing gear is directly related to the strut stroke and the square of the strut-stroking velocity, the variations of the two main-gear and nose-gear axial forces are essentially the same shape as the strokes. (Compare figs. 3(k), 3(l), and 3(m) to figs. 3(h), 3(i), and 3(j).) The higher frequency oscillations in the axial strut forces are primarily the result of the input disturbances from the runway roughness. The right-main-gear force for the coupled rudder-nosewheel landing is higher than that for rudder control only because of the larger induced rolling motions resulting from the greater inertial loading effects from airplane response to the coupled steering. Conversely, the left-main-gear forces are lower, due to inertial unloading effects, for the landing with coupled steering.

Crosswind Landings on Runway Center Line

Additional capabilities of the nosewheel steering option of the FATOLA computer program are illustrated by the analytical results presented in figure 4. Computed nosewheel steering angles, nosewheel yaw angles, airplane pitch attitudes, pitch rates, nosewheel steering forces, airplane c.g. position on runway, strut strokes, and axial strut forces are given for two landings on the runway center line. Landings under a steady 7.62 m/sec (25 ft/sec) left-to-right crosswind were simulated with no directional control and with nosewheel autopilot steering (based on lateral position on the runway and lateral drift-rate feedback). The solid curves in figure 4 are results for which the effects of the main-gear tire side forces due to yawed rolling are also included in the simulation.

Nosewheel steering angle.- Time histories of the nosewheel steering angles are presented in figure 4(a). As input, the steering angles are zero when no directional control is attempted. For the runs with directional control the autopilot tries to maintain the center line of the runway within a lateral tolerance band of ±9.14 m (±30 ft). For these runs the steering angle exhibits a sawtooth variation. When the main-gear tire side forces are included in the simulation the peak magnitudes of the nosewheel steering angle are somewhat reduced and the nosewheel steering corrections occur more frequently. Thus, including the main-gear tire side forces improves the response characteristics of the nosewheel steering option in FATOLA.

Nosewheel yaw angle.- Analytical variations of the nosewheel yaw angle for the crosswind landings on the runway center line are given in figure 4(b). When no directional control was attempted, the small nosewheel yaw angles shown are introduced by the airplane yaw. As expected for autopilot steering, the nosewheel yaw angles are similar to the steering angles for both cases, with and without the inclusion of main-gear tire side forces.

Pitch attitude.- Time histories of airplane pitch attitude are presented in figure 4(c). The data indicate no major differences in pitch attitude for the two steering conditions. Furthermore, the inclusion of main-gear side forces has little effect on airplane pitch attitude.

Pitch rate.- The airplane pitch-rate time histories are presented in figure 4(d). These data indicate that airplane pitch rate is also insensitive to the steering maneuvers and to the inclusion of the main-gear side forces for the landings that were considered.

Nosewheel steering force.- Variations in the nosewheel steering forces (fig. 4(e)) are similar, as they should be, to the variations of the yaw angles (fig. 4(b)). The positive and negative variations of the force for the autopilot steering landing are in phase with the steering angles commanded by the autopilot which attempts to maintain the location of the airplane within the lateral runway tolerances set in the autopilot.

Airplane c.g. runway position.- The airplane c.g. lateral position for the two crosswind landings is presented in figure 4(f). Without directional control the airplane quickly yawed into the wind and eventually ran off the left side of the runway. With nosewheel autopilot steering the airplane position was maintained within ±9.14 m (±30 ft) of the runway center line throughout the time history. Inclusion of the main gear tire side forces resulted in less cross-range excursions of the airplane.

Strut stroke.- Strut-stroke time histories are presented in figures 4(g) to 4(i) for the crosswind landing conditions. When no steering correction is attempted the right main gear strokes more than the left main gear, as expected, because of the roll moments created by inertial loading due to yaw-angle changes induced by the crosswind. When steering corrections are input by the autopilots the right- and left-main-gear strut strokes become oscillatory and are approximately 180° out of phase with each other. These same trends are also observed when the main-gear side forces are included in the simulation. The nose-gear strut strokes are relatively unaffected by autopilot steering maneuvers. How-

ever, drag parachute deployment decreases the nose-gear strokes for all three cases.

Axial strut force.- The axial strut forces for the right main, left main, and nose gears for the crosswind landings with no directional control and autopilot steering are presented in figures 4(j) to 4(l). The variations of the forces are similar to the strut-stroke variations shown in figures 4(g) to 4(i) because of the interrelationship of the strut strokes and axial strut force discussed previously. These load variations are the result of the airplane yaw and roll motions introduced by the steering controls.

Crosswind Landings off Runway Center Line

Limited analytical data for two additional landings are presented in figure 5 to illustrate further the steering capabilities in FATOLA. The figure shows comparisons of the computed nosewheel steering angles, nosewheel yaw angles, and airplane c.g. runway position for the touchdowns 16.8 m (55 ft) right and -16.8 m (-55 ft) left of the runway center line with nosewheel autopilot steering only under a 7.62-m/sec (25-ft/sec) crosswind from the left. For these cases the main-gear tire side forces were not included in the simulation. The basic airplane loads, strokes, and motions were essentially the same as those for the airplane landing on the runway center line; therefore, these data are not presented.

Nosewheel steering angle.- The nosewheel steering angles for the touchdowns ±16.8 m (±55 ft) right and left of the runway center line with the crosswind are shown in figure 5(a).

Although touchdowns were on opposite sides of the runway center line, the initial steering angles are in the same direction for both cases, however, the peak amplitude of the steering angle for the landing 16.8 m (55 ft) right of the center line is smaller and occurs earlier than for the corresponding case -16.8 m (-55 ft) left of the center line. The apparent anomaly of the initial steering angle in the same direction as the crosswind (for both landings) occurs because the steering autopilot utilizes both lateral drift rate with lateral feedback time constant (20 sec) and lateral position for determining control inputs. For the landing to the right of the center line, the yaw of the airplane into the wind introduced sufficient lateral drift rate to the left which, coupled with the 20-sec time constant, anticipates an excursion beyond the left error tolerance and causes the autopilot to steer right for correction even though the airplane was already to the right of the center line and out of the right error tolerance.

Nosewheel yaw angle.- As would be expected, the nosewheel yaw angles (fig. 5(b)) exhibit the same trends in amplitude and variation with time as did the steering angles (fig. 5(a)).

Airplane c.g. runway position.- Figure 5(c) presents the airplane c.g. position for the landing to the right and to the left of the runway center line under the 7.62-m/sec (25-ft/sec) crosswind. The data indicate that for both landings the autopilot nosewheel steering maintained the airplane position

within the runway boundaries and was generally steering the airplane closer to the runway center line during the landing roll-out.

CONCLUDING REMARKS

Modifications, including nosewheel steering, to improve the analytical capabilities of a muti-degree-of-freedom flexible aircraft take-off and landing analysis (FATOLA) computer program are presented, and supplemental instructions are included in an appendix for users of the FATOLA computer program. To illustrate several features and capabilities of an added nosewheel steering option, analytical results were obtained for conditions that included (1) rudder control only; (2) rudder-control deflections and nosewheel steering angles automatically coupled; (3) nosewheel autopilot steering, under a steady crosswind; and (4) no directional control, under a steady crosswind. The analytical results from these landing cases and steering situations indicate logical and consistent behavior of all of the airplane tracking, attitude, motions, and loads.

Langley Research Center
National Aeronautics and Space Administration
Hampton, VA 23665
October 25, 1978

APPENDIX A

SUPPLEMENTAL USER INSTRUCTIONS

To use the FATOLA computer program the reader will need reference 4 for the original rigid-body program (TOLA) and references 6 and 7 for the program with flexibility effects (FATOLA). The bulk of the required input data to use FATOLA is described in these references. However, the following new inputs associated with the modifications to the FATOLA program presented in this report are needed. The quantity, units, symbol, nominal value, and definition are listed under headings which identify the area of modification in the program to which the data are related. The format of the inputs can be found in Section III, entitled "Data Format," of reference 4.

Quantity	Units	Symbol	Nominal value	Definition
Landing-gear data:				
----	m (ft)	SLEN1	0.	Array of distances between upper and lower bearing for fully extended gear, maximum of 5
----	m(ft)	SLEN2	0.	Array of distances between hub and lower bearing for fully extended gear, maximum of 5
Strut air pressure equations:				
γ	----------	GAMA	1.	Ratio of specific heat at constant pressure to specific heat at constant volume
Strut vapor pressure:				
----	m^2 (ft^2)	AH	1.	Hydraulic area of each strut
Flexible-body modal damping data:				
----	$\frac{\text{N-sec}}{\text{m}}\left(\frac{\text{lbf-sec}}{\text{ft}}\right)$	GDAMP	0.	Array of modal damping values for each flexible mode used in analysis, maximum of 20

Quantity	Units	Symbol	Nominal value	Definition
Nosewheel steering data:				
----	----------	INDNWS	0	Nosewheel steering option indicator: 0 - No steering computed 1 - Compute steering
----	----------	IRUDD	0	Yaw autopilot indicator: 0 - Normal autopilot rudder variations 1 - Programmed (input) rudder variations
----	----------	INWRUD	0	Coupling yaw autopilot indicator: 0 - Programmed (input) rudder variation (IRUDD must also be 1) 1 - Path for automatic coupling of rudder deflections and nosewheel steering angle
η	deg	ETANOS	0.	Initial value of nosewheel angle for the steering input.
η_d	deg	ETADES	0.	Computed nosewheel steering angle
$\dot{\eta}_d$	deg/sec	ETART1	0.	Steering-angle rate of change
η_{max}	deg	ETAMAX	0.	Maximum limit, right nosewheel steering angle
η_{min}	deg	ETAMIN	0.	Minimum limit, left nosewheel steering angle
----	----------	PCTETA	1.	Factor on side force (FGPY) to give side force on nosewheel
KA	----------	KANWS	0	Indicator for yaw-angle steering control: 0 - No angle control 1 - Angle steering control
KP	----------	KPNWS	0	Indicator for lateral-position steering control: 0 - No position steering control 1 - Lateral-position steering control

Quantity	Units	Symbol	Nominal value	Definition
Nosewheel steering data:				
----	----------	ISTER	0	Steering indicator: 0 - Constant nosewheel angle 1 - Programmed (input) steering
R_ψ	sec	RPSI	0.	Positive rate feedback constant on angle steering control
ψ_d	deg	PSIDES	0.	Desired angle, airplane-runway center line for angle control steering
R_y	sec	RYR	0.	Positive rate feedback constant on position steering control
Y_{RD}	m (ft)	YRDES	0.	Desired lateral runway position in steering control
----	deg or m (ft)	EA	0.	Allowed error in airplane angle (KANWS = 1), or position (KPNWS = 1) for automatic steering
----	----------	CONFRI	0.	Constant in equation for side (yawed rolling) coefficient of friction for nosewheel (must be input as nonzero)
----	----------	CONFRM	0.	Constant in equation for side (yawed rolling) coefficient of friction for all main-gear wheels (must be input as nonzero)
----	----------	DELPWR	0.	Exponent on nosewheel yaw angle in side-friction equation
----	----------	DELPRM	0.	Exponent on all main-gear wheel yaw angles in side-friction equation
----	----------	VPOWR	0.	Exponent on nosewheel axle velocity in side-friction equation
----	----------	VPOWRM	0.	Exponent on all main-gear wheel-axle velocities in side-friction equation

Quantity	Units	Symbol	Nominal value	Definition
Nosewheel steering data:				
----	$\frac{N}{deg\ m}\left(\frac{lbf}{deg\ ft}\right)$	CONE	0.	Constant in cornering-power equation for nosewheel steering $CONE = 1.2C_c(p + 0.44p_r)\frac{w^2}{d}$
----	$\frac{N}{deg\ m}\left(\frac{lbf}{deg\ ft}\right)$	CONEM	0.	Constant in cornering-power equation for all main-gear wheels $CONEM = 1.2C_c(p + 0.44p_r)\frac{w^2}{d}$
----	$\frac{N}{deg\ m^2}\left(\frac{lbf}{deg\ ft^2}\right)$	CTWO	0.	Constant in cornering-power equation for nosewheel steering $CTWO = 8.8C_c(p + 0.44p_r)\frac{w^2}{d^2}$
----	$\frac{N}{deg\ m^2}\left(\frac{lbf}{deg\ ft^2}\right)$	CTWOM	0.	Constant in cornering-power equation for all main-gear wheels $CTWOM = 8.8C_c(p + 0.44p_r)\frac{w^2}{d^2}$
----	$\frac{N}{deg}\left(\frac{lbf}{deg}\right)$	CTHREE	0.	Constant in cornering-power equation for nosewheel steering $CTHREE = 0.0674C_c(p + 0.44p_r)w^2$
----	$\frac{N}{deg}\left(\frac{lbf}{deg}\right)$	CTHREM	0.	Constant in cornering-power equation for all main-gear wheels $CTHREM = 0.0674C_c(p + 0.44p_r)w^2$
----	$\frac{N}{deg\ m}\left(\frac{lbf}{deg\ ft}\right)$	CFOUR	0.	Constant in cornering-power equation for nosewheel steering $CFOUR = 0.34C_c(p + 0.44p_r)\frac{w^2}{d}$

Quantity	Units	Symbol	Nominal value	Definition
Nosewheel steering data:				
----	$\frac{N}{deg\ m}\left(\frac{lbf}{deg\ ft}\right)$	CFOURM	0.	Constant in cornering-power equation for all main-gear wheels $CFOURM = 0.34C_c(p + 0.44p_r)\frac{w^2}{d}$

The last eight symbols defined above are derived from equation (82) of reference 12 and utilize the parameters:

C_c = 1.1 for tire Type I
1.2 for tire Type III
1.0 for tire Type VII
1.0 for all others

where

w maximum width of undeflected tire

d outside diameter of free tire

p tire inflation pressure (in psi)

p_r tire rated inflation pressure (in psi)

In FATOLA the nose gear must be the first gear in the program such that I = 1 corresponds to the nose gear. If coupled rudder-nosewheel steering is used, the upper and lower limits on the rudder, DELRU and DELRL, and the upper and lower limits on the nosewheel steering angle, ETAMAX and ETAMIN, must be input. This option also requires that both IRUDD and INWRUD be input as 1. All steering options, except the completely automatic steering, make extensive use of the staging capabilities (see ref. 4) in FATOLA to insert the steering inputs at appropriate times.

The following example illustrates the procedure for determining the constant CONFRI,CONFRM, and the exponents DELPWR,DELPRM,VPOWR, and VPOWRM used in the expression for the side (yawed rolling) coefficient of friction, SIDEMU, programmed in FATOLA (see "Nosewheel Steering" section of appendix B).

To determine the constants CONFRI,DELPWR, and DELPRM, side-friction data from reference 13 were plotted on log-log graph paper as a function of wheel yaw angle for a constant velocity as indicated in sketch (a). A best-fit straight line drawn through the data points is of the form

$$y = ax^m$$

thus a and m or in this case CONFRI and DELPWR or DELPRM may be readily determined.

Similarly, the side-friction data were again plotted on log-log paper as a function of velocity for a constant yaw angle as illustrated in sketch (b) to determine the constants VPOWR or VPOWRM. In this case the exponent on velocity may be negative. Velocity effects on side friction generally occur on damp or flooded runways and are usually insignificant for dry runways. In the case where the side friction depends upon both tire yaw angle (DELN) and axle velocity (VAXLE) and their respective exponents, evaluating the two empirical expressions to obtain a combined new constant value for CONFRI allows determination of SIDEMU as $y = ax^m z^n$ (see appendix B) or

```
SIDEMU = CONFRI*(ABS(DELN))**DELPWR*(VAXLE)**VPOWR
```

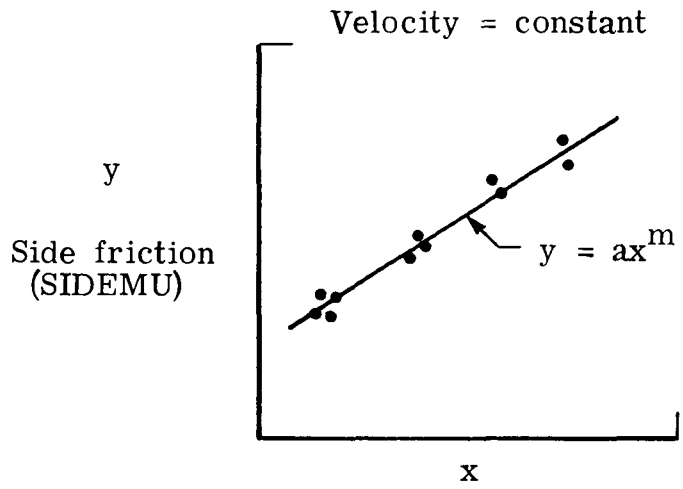

Sketch (a)

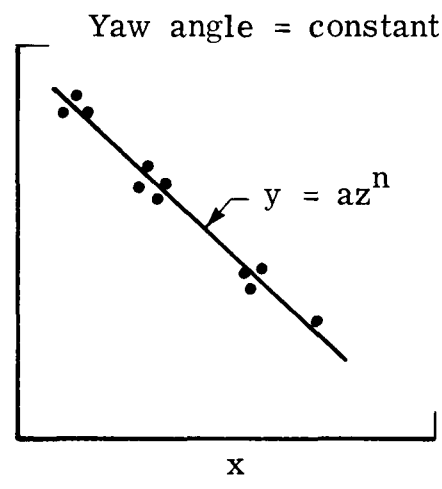

Sketch (b)

APPENDIX B

PROGRAMMING CHANGES

This appendix gives the changes in the FATOLA program to improve the analytical simulation capabilities. The modifications of reference 8 and the new input format have been incorporated into the present changes which allow all new input data to be part of the normal FATOLA data deck.

Strut Axial Friction

Three modifications were made to improve the simulation of the strut axial friction force. To accomplish the first two modifications, the following statements were inserted in the LGEA3C subroutine of FATOLA:

```
      DIMENSION IFRI(5)
      DATA (IFRI(I),I=1,5)/0,0,0,0,0/
      DATA RADDEG,DEGRAD/57.2957795,.01745329/
      IF(SD1(1,I).EQ.0.0.AND.IFRI(I).EQ.1)IFRI(I) = 0
      IF(SD1(1,I).LE.0.5.AND.IFRI(I).EQ.0)2,3
    2 HYPTAN = 1.0
      GO TO 4
    3 HYPTAN = ABS(TANH(4.0*SD1(1,I)))
      IFRI(I) = 1
    4 FF(I) = MUS(I)*SQRT(FDX(I)*FDX(I)+FDY(I)*FDY(I))
      FF(I) = FF(I)*(1.+2.*((SLEN2(I)-S(1,I))/(SLEN1(I)+S(1,I))))*HYPTAN
```

The DIMENSION statement sizes the friction indicators IFRI(I), and the DATA statement initializes the indicators to zero. The two IF statements and HYPTAN = 1.0 allow the full friction force to be used until the strut velocity SD(1,I) of any strut drops below 0.152 m/sec (0.5 ft/sec) (arbitrarily chosen) after the initial stroking. When the strut velocity becomes less than 0.152 m/sec (0.5 ft/sec), the friction force is transitioned through zero along the hyperbolic tangent function HYPTAN = ABS(TANH(4.0*SD1(1,I))).

The original strut axial friction-force equation (statement numbered 4) was modified to a form of equation (4) from reference 9 to include the moment effects on the axial friction. The expression is

$$FF(I) = FF(I)*((SLEN2(I)-S(1,I))/(SLEN1(I)+S(1,I)))$$

where

SLEN2(I) array of distances between hub and lower bearing for fully extended gear

SLEN1(I) array of distances between upper and lower bearing for fully extended gear

S(1,I) strut strokes for each gear

The third modification was to change the statement TMP(2) = 0.0 in the subroutine LGEAR1 to TMP(2) = 1.0, which allows the friction force to be effective at all times.

Strut Air Pressure Equations

Revised strut air pressure equations were also inserted in the LGEA3C subroutine to replace the original equations. The revised equations are

```
 P(I) = (PZERO(I)+PA77P)*(VZERO(I)/(VZERO(I)+A2(I)*S2(1,I)-
*S(1,I)*A(I)))**GAMA-PA77P
 P2(I) = (P20(I)+PA77P)*(V20(I)/TMP(1))**GAMA-PA77P
```

where PA77P (atmospheric pressure computed by the program) has been included to convert gage pressure to absolute pressure and GAMA(γ) has been added to allow variations in the compression process. The statement EQUIVALENCE(DM18(31),PA77P) was added to make the atmospheric pressure PA77P available in the subroutine.

Strut Vapor Pressure

To accommodate the condition of vapor pressure of the hydraulic fluid and its effect on the shock-strut force, the following changes were added to the LGEAR1 subroutine of FATOLA:

```
      IF(SD1(1,I).NE.0.)TMP(2)=SD1(1,I)/ABS(SD1(1,I)) (Existing statement)
      IF(P2(I).GT.0.)GO TO 1000
      PH(I)=(P(I)*AH(I)-FC2(I))/AH(I)
      IF(PH(I).LE.-1600.)GO TO 1003
1000  SF(I)=-P(I)*(A(I)-A2(I))-P2(I)*A2(I)+FC2(I)-S2D1(1,I)*
     C(C2(I)*ABS(S2D1(1,I))+C2L(I))-FF(I)*TMP(2)
      GO TO 1002
1003  SF(I)=-P(I)*(A(I)-AH(I))+1600.*AH(I)-FF(I)*TMP(2)
1002  IF(SD1(1,I).EQ.0.0.AND.FT(I).LE.ABS(SF(I)))SF(I)=-FT(I)
```

If the strut has two air chambers, the normal path in the program is followed. For a single-air-chamber strut, the hydraulic pressure is computed, a check is made to determine if vapor pressure has occurred, and the appropriate shock-strut force is computed based upon the hydraulic pressure conditions in the strut.

Structural Damping

Structural damping in the flexible-body simulation was incorporated by adding the expression

```
 GTF(IG)=GQ(IG)*GMASS1(IG)*GFREQ(IG)**2.
*          +GQD1(IG)*GDAMP(IG)
```

to the subroutine FLEX1 of the FATOLA program. The second term of the expression GQD1(IG)*GDAMP(IG) represents the modal damping force that has been added.

APPENDIX B

As stated in reference 11, the equivalent viscous form of structural damping GDAMP(IG) can be approximated by

$$GDAMP(IG) = K_{jj}g_j/\omega_j$$

where

K_{jj} jth generalized modal stiffness

g_j structural damping in jth mode (usually based on experimental data)

ω_j jth vibration natural frequency

Roll and Yaw Autopilots

The logic in the roll autopilot (fig. B-1) and control response sections were altered in the auxiliary computations routine of the program to permit variations in roll-control deflections to be simulated throughout the landing. For the roll autopilot the changes added after the "GO TO 103" statement were

```
102  IF(IAP.EQ.4)GO TO 78
     DELPDE = 0.0
     GO TO 103
 78  IF(TR.LE.TST)GO TO 68
     TMP5 = DELA*(TR-TST)
     DELPDE = DELPI + TMP5
     GO TO 103
 68  DELPI = DELPD
     GO TO 103
```

and in the control response

```
 63  IF(IAP.EQ.4)GO TO 64
```

The changes given create, in the roll autopilot, a special branch for the landing impact and roll-out phase (IAP = 4) to allow the aileron deflections to be initialized and programmed by inputs of DELPD (initial input aileron deflection), TST (time for staging), and DELA (aileron rate). The addition of statement 63 in the control response also switches the logic only for IAP = 4 to set the actual aileron deflection, used elsewhere in the program, to the desired value of aileron deflection (DELPDE) computed in the roll autopilot.

To allow programmed rudder-control variations similar to the roll autopilot and to provide a path for automatic coupling of rudder deflections and nosewheel steering angle, the yaw autopilot was modified as follows:

```
     CALL SACS11
 34  IF(IAP.GT.2)GO TO 500
     DELRN=DELRNN
     BETAE=BETAD
     BETAET=BETAE+RFB*BETAR1*RADDEG
     DELRDE=DELRN
```

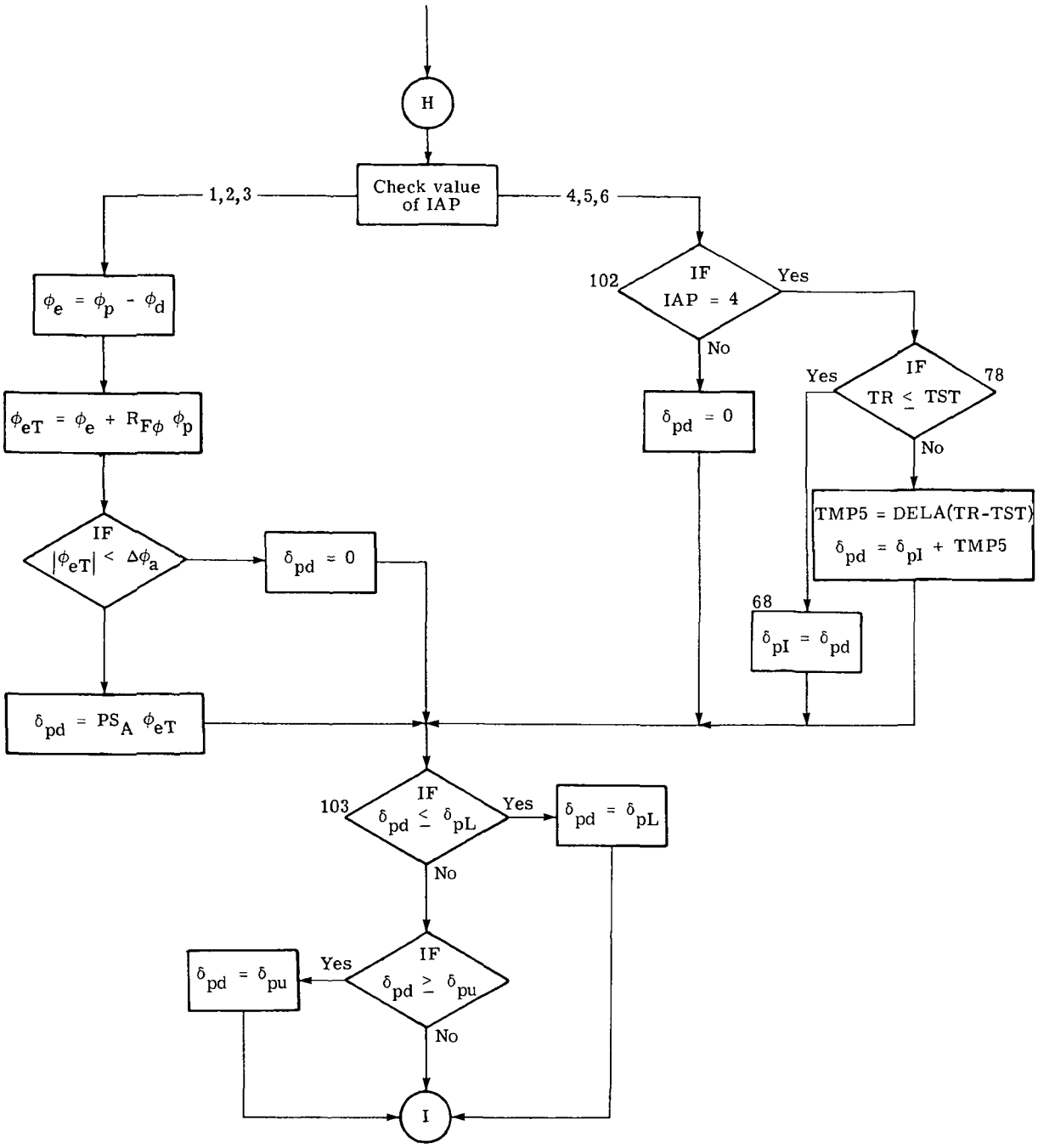

Figure B-1.- Roll autopilot logic.

```
      IF(ABS(BETAET).GE.DELBA)DELRDE=DELRN+PSR*BETAET
      GO TO 101
  500 IF(IRUDD.EQ.1)GO TO 5
      GO TO 150
    5 IF(INWRUD.EQ.1)GO TO 6
      IF(TR.LE.TST)GO TO 27
      DELRDE=DELRDI+DELRRD*(TR-TST)
      GO TO 101
   27 DELRDI=DELRD
      GO TO 101
  150 DELRN=DELRNN
      PSIE=PSIPD
      PSIET=PSIE+RFPSI*PSIPD1*RADDEG
      DELRDE=DELRN
      IF(ABS(PSIET).GE.OPSIA)DELRDE=DELRN+PSPSI*PSIET
      GO TO 101
    6 IF(TR.LE.TST)GO TO 110
      DELRDE=DELRDI+DELRRD*(TR-TST)
      GO TO 101
  110 IF(ABS(DELRDE).GT.0.0)GO TO 120
      DELRDI=DELRD
      GO TO 101
  120 DELRDI=DELRDE
  101 IF(DELRDE.LT.DELRL)DELRDE=DELRL
      IF(DELRDE.GT.DELRU)DELRDE=DELRU
      IF(IPR.EQ.0)CALL AUTPR6
  106 CONTINUE
```

where

IRUDD = 0 indicates autopilot rudder variations

= 1 indicates programmed (input) variations

INWRUD = 0 indicates programmed (input) variations (IRUDD must be 1)

= 1 indicates rudder variations are automatically coupled to the nosewheel for steering control

All other variables are defined in FATOLA. The complete yaw autopilot logic is illustrated in figure B-2.

Changes also made in the control-response section of the AUTS subroutine to allow rudder variations to be input included the insertion of

```
      IF(IRUDD.EQ.1)GO TO 49
      IF(DELRDE.LT.DELRD)DELRD1=-DELRRD
   49 DELPD1=DFLA
```

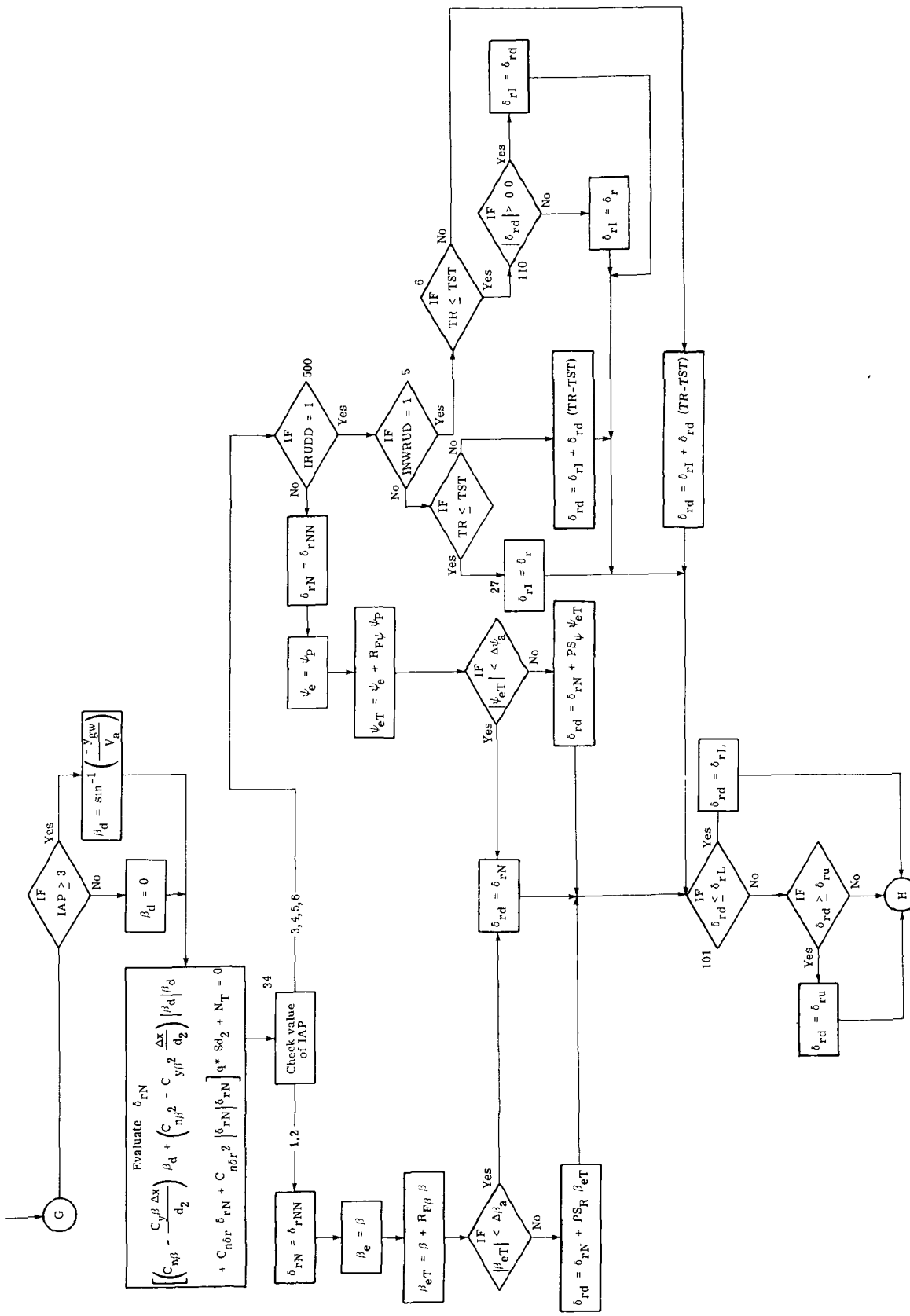

Figure B-2.- Yaw autopilot logic.

after DELRD1 = DELRRD and

```
 61  IF(IAP.EQ.4)GO TO 62
     IF(ABS(DELRD1*DELTS).GE.ABS(DELRDE-DELRD))GO TO 62
```

after statement 60.

Nosewheel Steering

The ground-plane forces for the nosewheel steering option were included by the following statements added to the indicated locations in the LGEAR1 and LGEA3C subroutines.

In LGEAR1 following the existing EQUIVALENCE statements add

```
EQUIVALENCE (INDSTE(73),PSIPD)
DATA RADDEG,DEGRAD/57.2957795,.01745329/
```

and following the IF statement after statement number 20 insert

```
IF(INDNWS.EQ.1.AND.I.EQ.1)GO TO 301
```

and after the

```
     GO TO 201
```

add

```
301   MA(I)=-FTRY(I)*TMP(1)*SIN((PSIPD+ETADES)*DEGRAD)+
     1   FTRX(I)*TMP(1)*COS((PSIPD+ETADES)*DEGRAD)
      GO TO 201
```

to account for the moment of the ground forces about the nosewheel axle for the nosewheel steering case.

After the computation of VTY(I) in LGEA3C add

```
      TMPETA = ETADES
      IF(I.EQ.1 .AND. INDNWS.EQ.1)GO TO 200
      TMPETA = 0.0
 200  IF(ABS(OMET(1,I)*TMP(1)*COS((PSIPD+TMPETA)*DEGRAD))
     1   .GE. (RG11*RDXG(I)+RG13*RDZG(I)))GO TO 201
      VTX(I)=VTX(I)-TMP(2)+OMET(1,I)*TMP(1)*COS((PSIPD+TMPETA)*DEGRAD)
      VTY(I) = RDYG(I)+OMET(1,I)*TMP(1)*SIN((PSIPD+TMPETA)*DEGRAD)
   7  VTZ(I)=RG31*RDXG(I)+RG33*RDZG(I)
      GO TO 203
 201  VTX(I)=1.E-10
      OMET(1,I)=-((RG11*RDXG(I)+RG13*RDZG(I))/(COS((PSIPD+TMPETA)*
     1    DEGRAD)))/(RZERO(I)-DELTA(I))
      VTY(I) = RDYG(I)+OMET(1,I)*TMP(1)*SIN((PSIPD+TMPETA)*DEGRAD)
      VTZ(I)=RG31*RDXG(I)+RG33*RDZG(I)
```

```
C      CALCULATION OF GROUND PLANE FORCES FTRX(I) AND FTRY(I)
  203 TMP(1)=RG11*RDXG(I)+RDZG(I)*RG13
```

and after statement number 53 add the side-force formulation (from ref. 12 pages 30 to 34).

```
      IF(I.GT.1)GO TO 41
      ETAVE=ATAN2(RDYG(I),TMP(1))
      DELN=PSIPD+ETADES-ETAVE*RADDEG
      IF(DELTA1 .EQ. 0.0) FGPY = 0.0
      IF(DELTA1 .EQ. 0.0)GO TO 48
      IF(DELN.EQ.0.0.OR.XG77F1.EQ.0.0)GO TO 110
      SIDEMU = CONFRI*(ABS(DELN))**DELPWR*VAXLE(I)**VPOWR
      GO TO 180
110   SIDEMU=1.0E-6
180   IF((DELTA1/2.*RZERO(I)) .GT. 0.0875)GO TO 130
      CRNPWR=CONE*DELTA1-CTWO*DELTA1**2.
      GO TO 170
130   CRNPWR=CTHREE-CFOUR*DELTA1
 170  YAWPRM=ABS(CRNPWR*DELN/(SIDEMU*FTRZ(I)))
      IF(YAWPRM.LE.1.5)GO TO 150
      FGPY=SIDEMU*FTPZ(I)*COS(DELN*DEGRAD)
      GO TO 160
150   FGPY=((YAWPRM-(4.0/27.0)*YAWPRM**3.0)*SIDEMU*FTRZ(I))
     1      *COS(DELN*DEGRAD)
160   FGPY=PCTETA*FGPY
      IF(DELN.GT.0.0)FGPY=ABS(FGPY)
      IF(DELN.LT.0.0)FGPY=-ABS(FGPY)
      DFTRX=FGPY*SIN(ETAVE)
      DFTRY=FGPY*COS(ETAVE)
      FTRX(I)=FTRX(I)+DFTRX
      FTRY(I)=FTRY(I)+DFTRY
      GO TO 48
```

Also after FTRY(I) = 0. at statement number 40 add

```
      IF(I .GT. 1)GO TO 48
      FGPY=0.0
      GO TO 48
   41 ETAVEM=ATAN2(RDYG(I),TMP(1))
      DELNM=PSIPD-ETAVEM*RADDEG
      IF(DELTA(I).EQ.0.0)FGPYM=0.0
      IF(DELTA(I).EQ.0.0)GO TO 48
      IF(DELNM.EQ.0.0.OR.XG77F1.EQ.0.0)GO TO 1100
      SIDMUM =CONFRM*(ABS(DELNM))**DELPRM*VAXLE(I)**VPOWRM
      GO TO 1800
1100  SIDMUM =1.0E-6
1800  IF((DELTA(I)/2.*RZERO(I)).GT.0.0875)GO TO 1300
      CRNPRM = CONEM*DELTA(I)-CTWOM*DELTA(I)**2.
      GO TO 1700
1300  CRNPRM = CTHREM-CFOURM*DELTA(I)
1700  YAWPMM = ABS(CRNPRM*DELNM/(SIDMUM*FTRZ(I)))
```

```
      IF(YAWPMM .LE.1.5)GO TO 1500
      FGPYM = SIDMUM*FTRZ(I)*COS(DELNM*DEGRAD)
      GO TO 1600
1500  FGPYM = ((YAWPMM-(4.0/27.0)*YAWPMM**3.0)*SIDMUM*FTRZ(I))
     1     *COS(DELNM*DEGRAD)
1600  IF(DELNM.GT.0.0)FGPYM=ABS(FGPYM)
      IF(DELNM.LT.0.0)FGPYM=-ABS(FGPYM)
      DFTRXM=FGPYM*SIN(ETAVEM)
      DFTRYM=FGPYM*COS(ETAVEM)
      FTRX(I)=FTRX(I)+DFTRXM
      FTRY(I)=FTRY(I)+DFTRYM
   48 CONTINUE
```

In the above formulation, the relationship of the nosewheel ground-plane force to the FATOLA runway and airplane coordinate systems is illustrated in sketch (c).

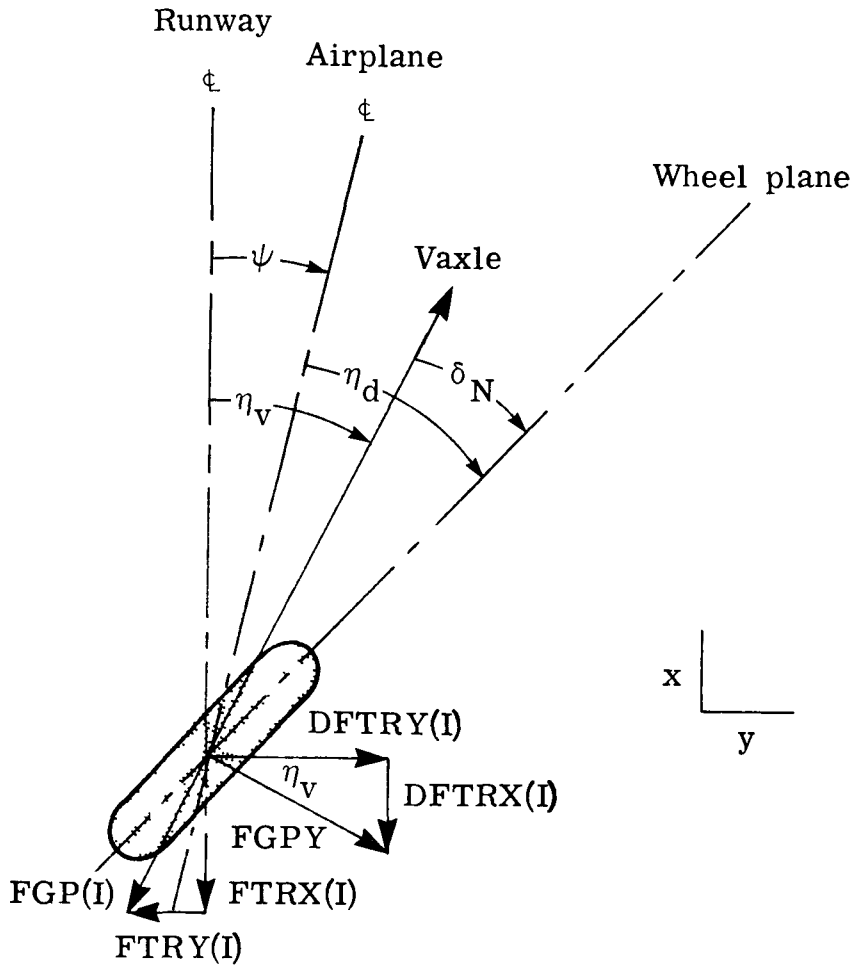

Sketch (c)

where new angles are defined as

$$\delta_N = \psi + \eta_d - \eta_V$$

$$\eta_V = \tan^{-1}(RDYG(I)/TMP(1)) \text{ (axle velocity components defined in program)}$$

and

δ_N(DELN) wheel yaw angle relative to axle velocity

ψ(PSIPD) airplane yaw angle (computed in FATOLA)

η_d(ETADES) desired nosewheel steering angle (η_d = 0.0 for main gears)

η_V(ETAVE) angle of the wheel-axle velocity vector relative to the runway center line

DFTRX(I), DFTRY(I) differential x- and y-direction ground-plane forces due to steering (to be added to present FTRX(I) and FTRY(I) in FATOLA)

The empirical formulations for yaw parameter (YAWPRM) and cornering power (CRNPWR), equations (80) and (82) in reference 12, have been utilized. To parallel the above formulation, friction data from reference 13 for yawed rolling tires on dry, wet, and flooded runway surfaces were analyzed to form the empirical expression for side or yawed rolling (SIDEMU) coefficient of friction. The equation form found to be $y = ax^m z^n$ (see appendix A) was programmed as SIDEMU = CONFRI*(ABS(DELN))**DELPWR*(VAXLE)**VPOWR for the nosewheel.

To accompany the nosewheel steering-side-force formulation, the following nosewheel steering autopilot was added after statement 1 in the AUTS subroutine.

```
      IF(DELTA1.EQ.0.0)GO TO 130
      IF(INDNWS.EQ.0)GO TO 8
      IF(KANWS.EQ.1)GO TO 7
C        CURRENTLY, NOSEWHEEL STEERING IS FOR DISTANCE ERROR
C                   NOT ANGLE ERROR
      IF(KPNWS.EQ.1)GO TO 9
  130 IF(ISTER.EQ.1)GO TO 29
      IF(INWRUD.EQ.1)GO TO 82
      GO TO 8
   82 IF(DELRDE.GT.0.0)GO TO 86
      ETADES = DELRDE*(ETAMAX/DELRL)
      GO TO 8
   86 ETADES = DELRDE*(ETAMIN/DELRU)
      GO TO 8
   29 IF(TR.LE.TST)GO TO 35
      ETADES=ETANOS+ETART1*(TR-TST)
      GO TO 31
   35 ETADES=ETANOS
      GO TO 31
    7 ERROR=(PSIPD-PSIDES)+RPSI*PSIPD1*RADDEG
      GO TO 3
    9 ERROR=(YR-YRDES)+RYR*YRD1
```

```
  3 IF(ILIM .EQ. 1 .AND. ETADES .EQ. 0.0) INOSE=0
    IF(INOSE .GT. 0 .AND. ETADES .EQ. 0.0) GO TO 8
    IF(ABS(ERROR) .GT. EA) GO TO 30
    GO TO 32
 30 IF(ERROR .GT. 0.0) GO TO 37
    ETADES=ETADES+ETART1*DELTS
    INCSE=1
    GO TO 31
 37 ETADES=ETADES-ETART1*DELTS
    INOSE=2
    GO TO 31
 32 IF(INOSE .EQ. 2) GO TO 38
    GO TO 39
 38 ETADES=ETADES+ETART1*DELTS
    ILIM=1
    GO TO 99
 39 ETADES=ETADES-ETART1*DELTS
    ILIM=1
 99 IF(ABS(ETADES) .LT. 1.0) ETADES = 0.0
 31 IF(ETADES .GT. ETAMAX) ETADES=ETAMAX
    IF(ETADES .LT. ETAMIN) ETADES=ETAMIN
  8 CONTINUE
```

In the autopilot five indicators determine the path for steering:

INDNWS
- 0 no nosewheel steering computations
- 1 compute nosewheel steering

KANWS
- 0 no angular control of steering
- 1 angular control-automatic steering

KPNWS
- 0 no position control of steering
- 1 position control-automatic steering

ISTER
- 0 constant nosewheel angle (last value computed)
- 1 programmed (input) nosewheel steering

INWRUD
- 0 programmed (input) rudder variations (IRUDD must equal 1)
- 1 programmed rudder variations automatically coupled to nosewheel

Figure B-3 illustrates the complete nosewheel steering autopilot logic.

New Input/Output Data

The new variables associated with the modifications to FATOLA are made available to the program subroutine where they are used by appropriate expansion of the COMMON/DIRCOM/ and other related modifications required in many of the subroutines of FATOLA. Most of the expansion of COMMON/DIRCOM/ was simply including dummy space at the end of the COMMON and listing only variables needed in the specific subroutines.

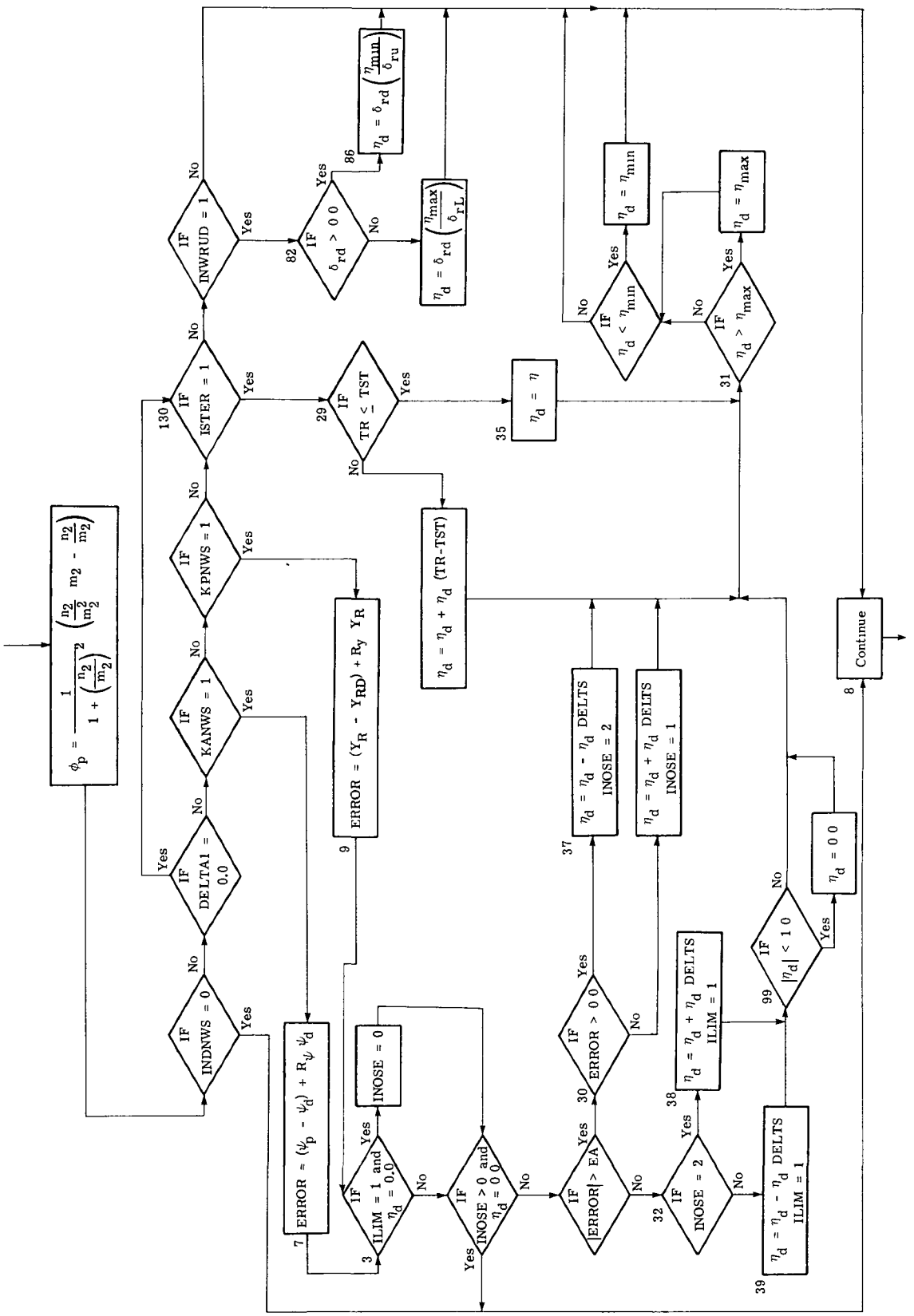

Figure B-3.- Steering autopilot logic.

In the subroutine EXE, for example, COMMON space was added as

```
*,DM64(30),GAMA,DM65(15),PCTETA,DM66(13),AH(5),DM67(35)
```

and statement 34 was altered to

```
34 DO 35 II=1,4036
```

to handle the initialization of the additional inputs. To assign nominal values to AH(I) and to PCTETA and GAMA the statements

```
   DO 30 I=1,5
30 AH(I)=1.0
```

were added after statement 24 and PCTETA = 1.0 and GAMA = 1.0 were added after INDATM = 1.

In subroutines INUPD, UPDAT, MIMIN, LGDET, STGTSI, STGTST, DEF, LINES, ERROR, EXERR, ATMS, TFFS1, TFFS8, TFFS9, VPCS1, SACS1, OPT1, FLARE1, AUTPR1, THAUTS, ENGFL, and CENGL only dummy space was required at the end of COMMON/DIRCOM/. In subroutine LGEAR1 the additional COMMON/DIRCOM/ space was added as

```
*,DDM21(43),INDNWS,DDM22(10),ETADES,DDM23(5),AH(5),PH(5),DDM24(30)
```

In subroutine LGEA3C the additional COMMON/DIRCOM/ space was added as

```
*,DDM30(20),SLEN1(5),SLEN2(5),GAMA,CFOUR,CONE,CONFRI,CTHREE,CTWO,
*DELPWR,DTIRE,DDM31(5),INDNWS,DDM32(2),PCTETA,DDM33(3),VPOWR,
*DDM34,FGPY,DELN,ETADES,DDM35(15),CONFRM,DELPRM,VPOWRM,CONEM,CTWOM,
*CTHREM,CFOURM,DDM36(23)
```

and in subroutine FLEX1 as

```
*,GDAMP(20),DDM25(80)
```

since the listed variables were required in the subroutines.

In the subroutine STORE the

```
COMMON/DIRCOM/DATA(4036)
```

replaces the existing COMMON statement to increase the space allocated to data to accommodate new inputs.

In the subroutine DSERCH, the COMMON was replaced with

```
COMMON/FIXDIR/ANAME(1000),LOC(1000),NCOUNT
```

and in the block data sections DIR0DA, DIR1DA, DIR2DA, and DIR3DA the COMMON was replaced with

```
COMMON/FIXDIR/NAME(1000),LOC(1000),NCOUNT
```

to increase the space for the names and locations of the new input data.

In DIR3DA it was also necessary to modify the data by including the name and location of all new inputs to the program. The replacements and/or changes included

```
DATA(NAME(K3),K3=876,936)/
```

and

```
*    6HPF     ,6HGQ     ,6HGQD1   ,6HGQD2   ,6HIFLX   ,6HGDAMP  ,6HSLEN1  ,
*    6HSLEN2  ,6HGAMA   ,6HCFOUR  ,6HCONE   ,6HCONFRI,6HCTHREE,6HCTWO   ,
*    6HDELPWP,6HDTIRE  ,6HEA     ,6HETAMAX,6HETAMIN,6HETANOS,6HETART1,
*    6HINDNWS,6HKANWS  ,6HKPNWS  ,6HPCTETA,6HPSIDES,6HRPSI   ,6HRYR    ,
*    6HVPOWR  ,6HYRDES  ,6HFGPY   ,6HDELN   ,6HETADES,6HILIM   ,6HINOSE  ,
*    6HISTER  ,6HIRUDD  ,6HINWRUD,6HAH     ,6HPH     ,6HCONFRM,6HDELPRM,
*    6HVPOWRM,6HCONEM  ,6HCTWOM  ,6HCTHREM,6HCFOURM/
 DATA(LOC(K4),K4=876,936)/
```

and in the locations block data

```
*    1892     ,1893     ,1894     ,1914     ,1934     ,2034     ,2134     ,
*    2234     ,2239     ,2319     ,2379     ,2499     ,2500     ,3700     ,
*    3760     ,3880     ,3900     ,3920     ,3940     ,3960     ,3980     ,
*    3985     ,3990     ,3991     ,3992     ,3993     ,3994     ,3995     ,
*    3996     ,3997     ,3998     ,3999     ,4000     ,4001     ,4002     ,
*    4003     ,4004     ,4005     ,4006     ,4007     ,4008     ,4009     ,
*    4010     ,4011     ,4012     ,4013     ,4014     ,4015     ,4016     ,
*    4017     ,4018     ,4019     ,4020     ,4025     ,4030     ,4031     ,
*    4032     ,4033     ,4034     ,4035     ,4036     /
```

The required addition of COMMON in the AUTS subroutine was to include and name in COMMON/DIRCOM/ the following variables:

```
*,DDM41(38),EA,ETAMAX,ETAMIN,ETANOS,ETART1,INDNWS,KANWS,KPNWS,
*DDM42,PSIDES,RPSI,RYR,DDM43,YRDES,DDM44(2),ETADES,ILIM,INOSE,
*ISTER,IRUDD,INWRUD,DDM45(40)
```

To both print and plot the nosewheel side force FGPY, the nosewheel control or yaw angle DELN, and the nosewheel steering angle ETADES associated with the new steering option, the following changes were made in the subroutine SDFLGP and the plotting program PLTDAT.

In subroutine SDFLGP the statement

```
C,DM18(52),FGPY,DELN,ETADES,DM19(45)
```

was added to the end of COMMON/DIRCOM/. The DIMENSION OP16(8) statement was altered to be

```
 DIMENSION OP16(18),OP17(8),OP18(8),OP19(7),OP20(8),OP21(8),
1    DAT2(18),DAT3(6),DAT4(15)
```

and the *(OP19(I),I = 1,4) statement of the DATA section was altered to be

```
*(OP19(I),I=1,7)/3HFZM,2HLM,2HMM,2HNM,4HFGPY,4HDELN,6HETADES/,
```

Also the DATA DAT1 statement was altered to be

```
DATA DAT1/4HTIME/,(DAT2(I),I=1,18)/2HLM,2HMM,2HNM,5HQI77R,
```

and the second continuation statement was changed to

```
*5HXG77F,5HYG77F,5HAX77F,6HXG77F1,4HFGPY,4HDELN,6HETADES/,
```

In addition, the DATA N1 statement was revised to

```
DATA N1/1/,N15/15/,N14/14/,N18/18/
```

After statement 201, a second continuation card was added to the IF(ISDF.NE.0)WRITE(13) statement as

```
2    ,FGPY,DELN,ETADES
```

and near statement 32 the CALL STFL and CALL STOVAR statements were changed to

```
CALL STFL(2,7,OP19)
CALL STOVAR(7,FZM,LM,MM,NM,FGPY,DELN,ETADES,DU)
```

The above changes in SDFLGP store the values of the new variables, print the headings and the values of the variables, and output the values of the variables to the plot tape for subsequent plotting.

Minor changes were also required in the PLTDAT plotting program of FATOLA to allow the new variables from the steering option to be plotted. The changes included altering the DIMENSION statement in PLTDAT to be

```
DIMENSION TITLE(18), BUF(400), NDIL(28), TBUF(400),
```

and changing statement 50 to be

```
50 DO 51 I=1,18
```

REFERENCES

1. McGehee, John R.; and Carden, Huey D.: A Mathematical Model of an Active Control Landing Gear for Load Control During Impact and Roll-Out. NASA TN D-8080, 1976.

2. Lynch, Urban H. D.: Takeoff and Landing Analysis (TOLA) Computer Program. Part I: Capabilities of the Takeoff and Landing Analysis Computer Program. AFFDL-TR-71-155, Part 1, U.S. Air Force, Feb. 1972. (Available from DDC as AD 741 942.)

3. Lynch, Urban H. D.; and Dueweke, John J.: Takeoff and Landing Analysis (TOLA) Computer Program. Part II.- Problem Formulation. AFFDL-TR-71-155, Part II, U.S. Air Force, May 1974.

4. Lynch, Urban H. D.; and Dueweke, John J.: Takeoff and Landing Analysis Computer Program (TOLA). Part III.- User's Manual. AFFDL-TR-71-155, Part III, U.S. Air Force, Apr. 1974.

5. Young, Fay O.; and Dueweke, John J.: Takeoff and Landing Analysis Computer Program (TOLA). Part IV: Programmer's Manual. AFFDL-TR-71-155, Part IV, U.S. Air Force, Jan. 1975.

6. Dick, J. W.; and Benda, B. J.: Addition of Flexible Body Option to the TOLA Computer Program. Part I - Final Report. NASA CR-132732-1, 1975.

7. Dick, J. W.; and Benda, B. J.: Addition of Flexible Body Option to the TOLA Computer Program. Part II - User and Programmer Documentation. NASA CR-132732-2, 1975.

8. Carden, Huey D.; and McGehee, John R.: Validation of a Flexible Aircraft Take-Off and Landing Analysis (FATOLA). NASA TP-1025, 1977.

9. Milwitzky, Benjamin; and Cook, Francis E.: Analysis of Landing-Gear Behavior. NACA Rep. 1154, 1953. (Supersedes NACA TN 2755.)

10. Wignot, Jack E.; Durup, Paul C.; and Gamon, Max A.: Design Formulation and Analysis of an Active Landing Gear. Volume I. Analysis. AFFDL-TR-71-80, Vol. I, U.S. Air Force, Aug. 1971. (Available from DDC as AD 887 127L.)

11. Edinger, Lester D.; Schenk, Frederick L.; and Curtis, Alan R.: Study of Load Alleviation and Mode Suppression (LAMS) on the YF-12A Airplane. NASA CR-2158, 1973.

12. Smiley, Robert F.; and Horne, Walter B.: Mechanical Properties of Pneumatic Tires With Special Reference to Modern Aircraft Tires. NASA TR R-64, 1960. (Supersedes NACA TN 4110.)

13. Yager, Thomas J.; and McCarty, John L.: Friction Characteristics of Three 30 × 11.5-14.5, Type VIII, Aircraft Tires With Various Tread Groove Patterns and Rubber Compounds. NASA TP-1080, 1977.

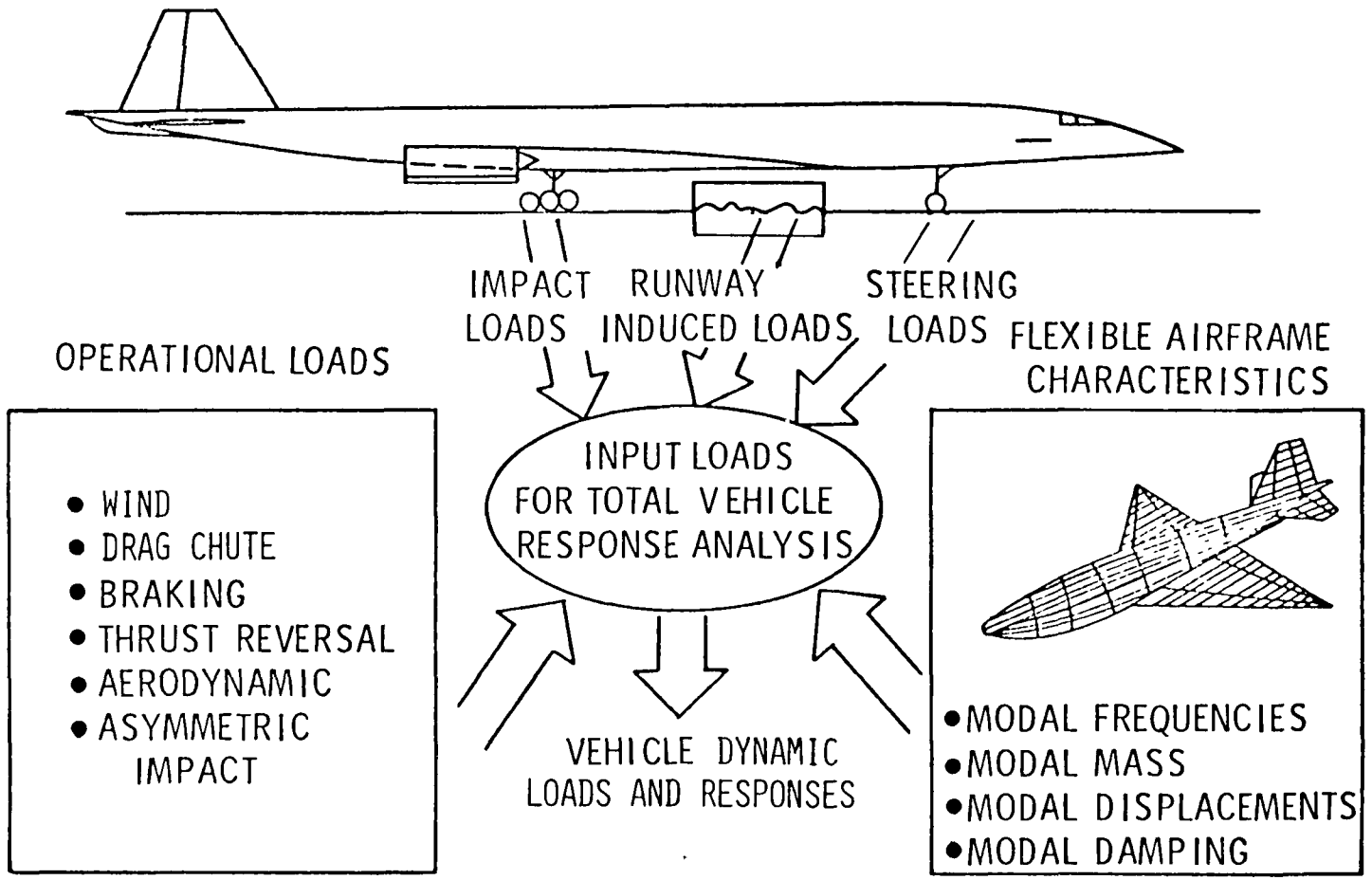

Figure 1.- General capabilities of flexible aircraft take-off and landing analysis (FATOLA) computer program.

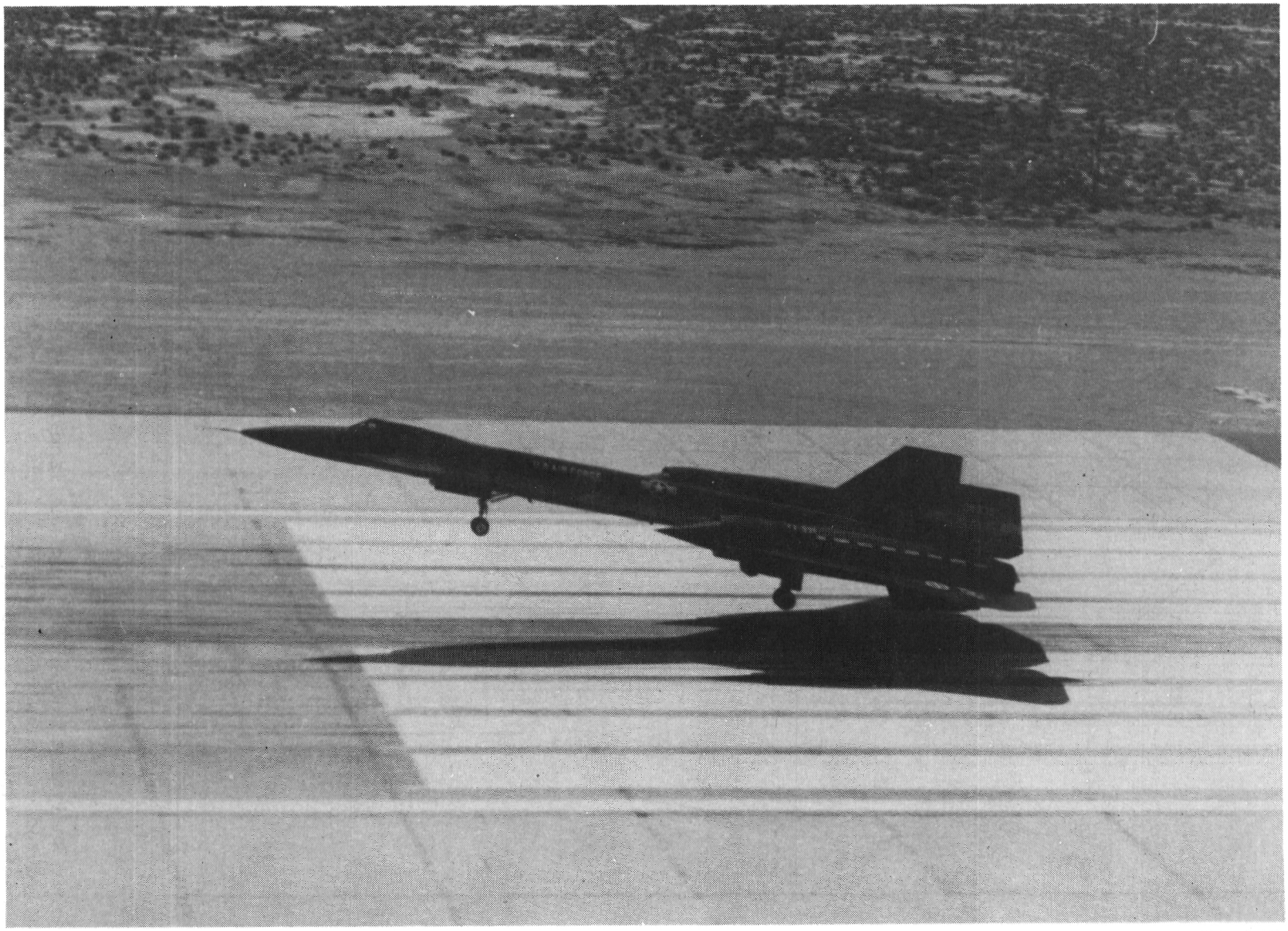

L-78-149

Figure 2.- Supersonic cruise research airplane.

SR-71

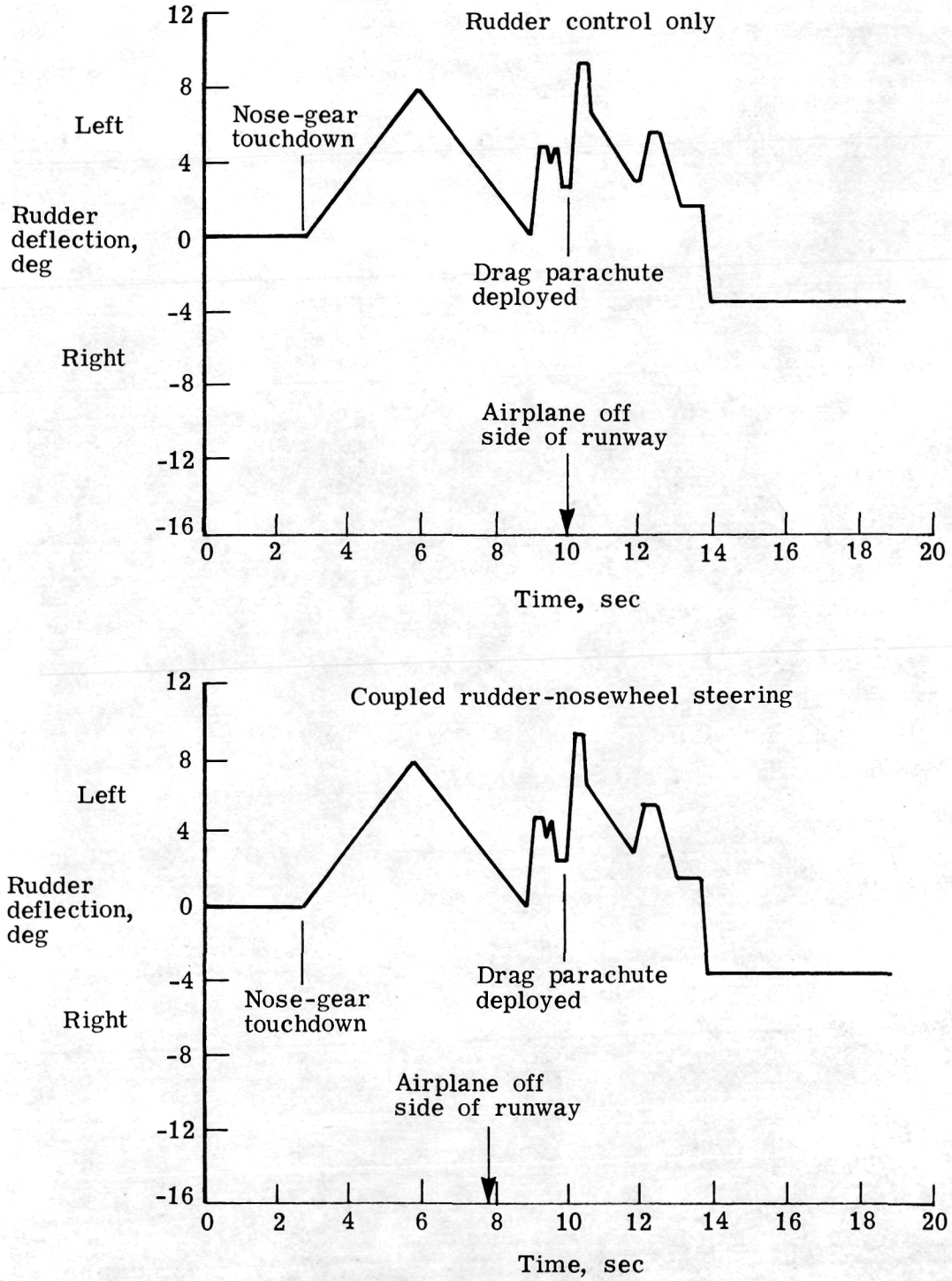

(a) Input rudder deflections.

Figure 3.- Analytical data for airplane landings with rudder control only and coupled rudder-nosewheel steering. Touchdown 16.8 m (55 ft) right of runway center line. No crosswind.

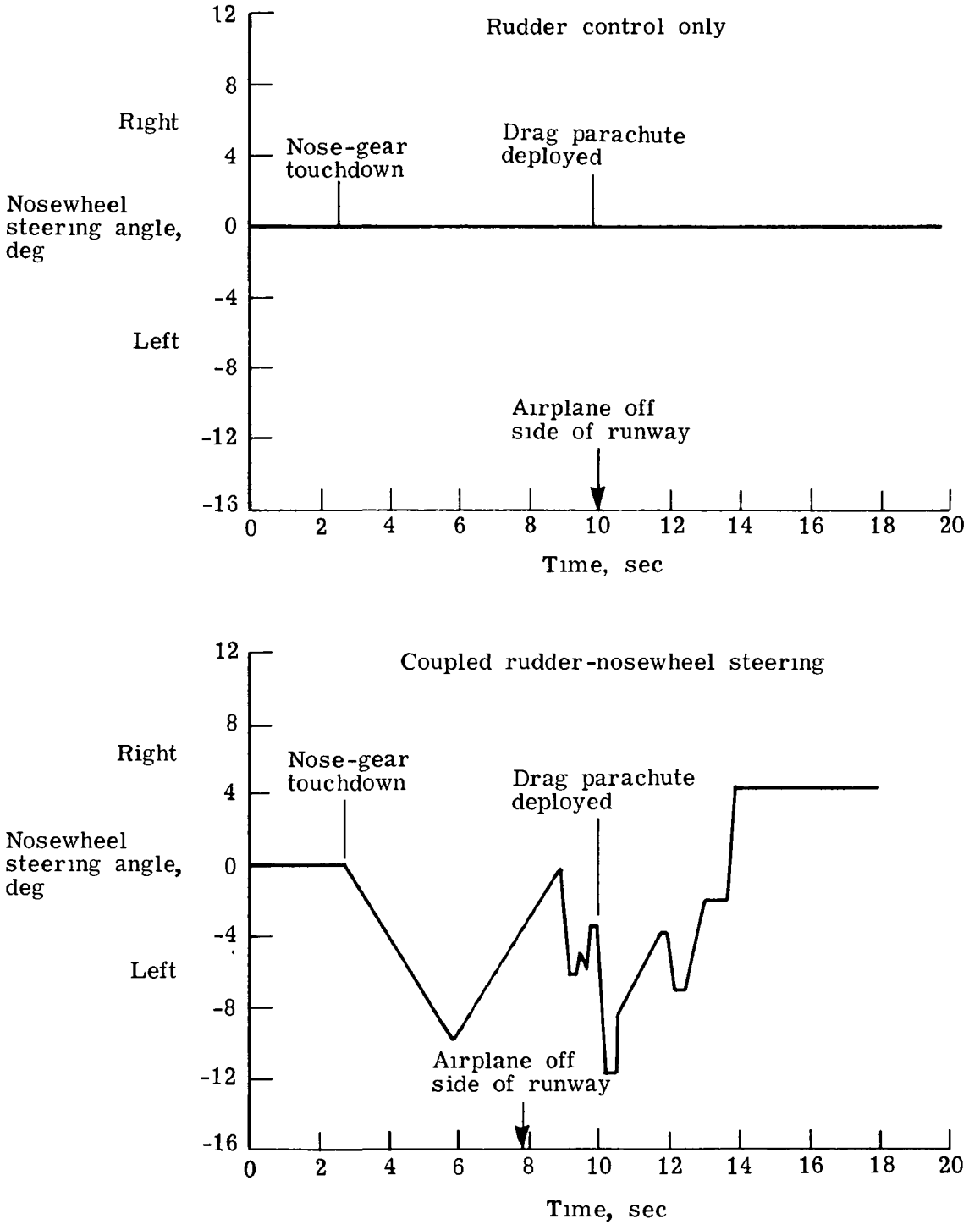

(b) Input nosewheel steering angles.

Figure 3.- Continued.

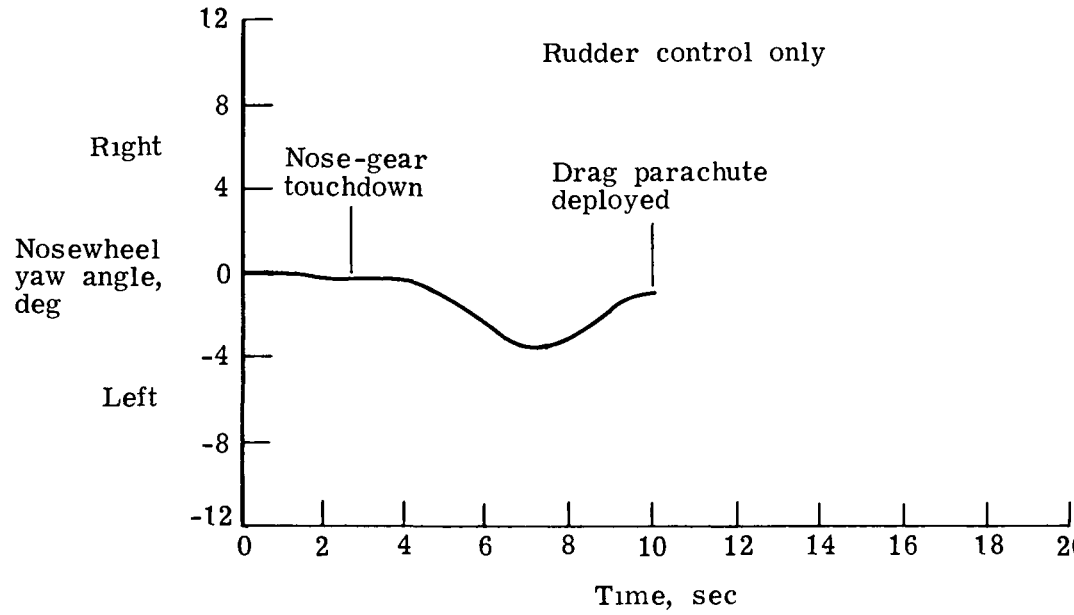

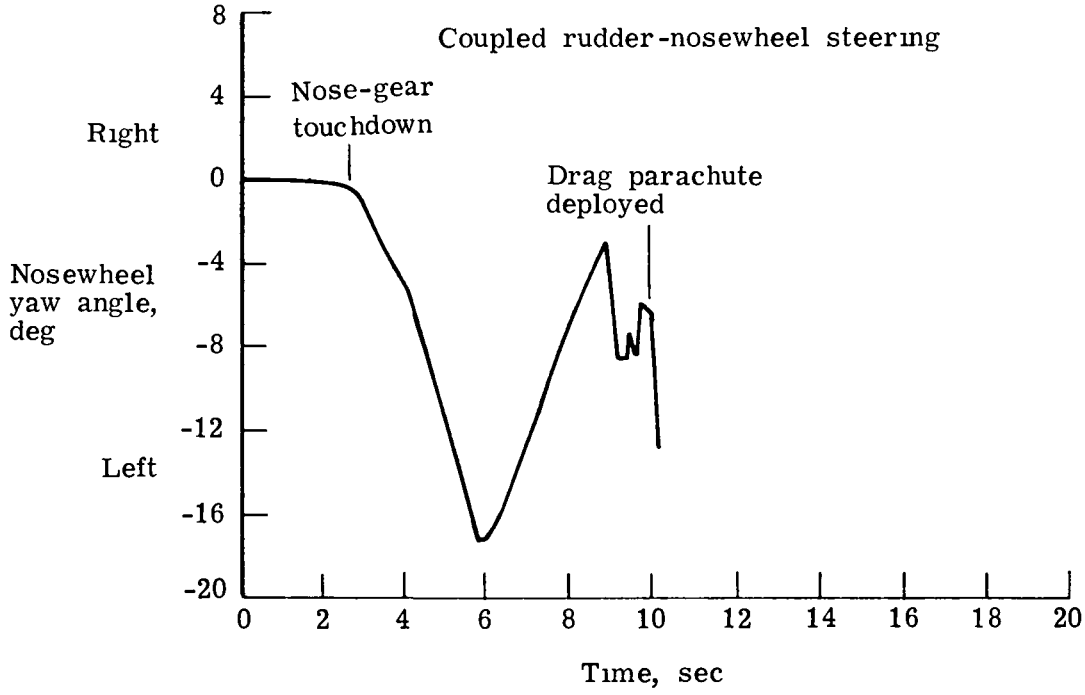

(c) Nosewheel yaw angles.

Figure 3.- Continued.

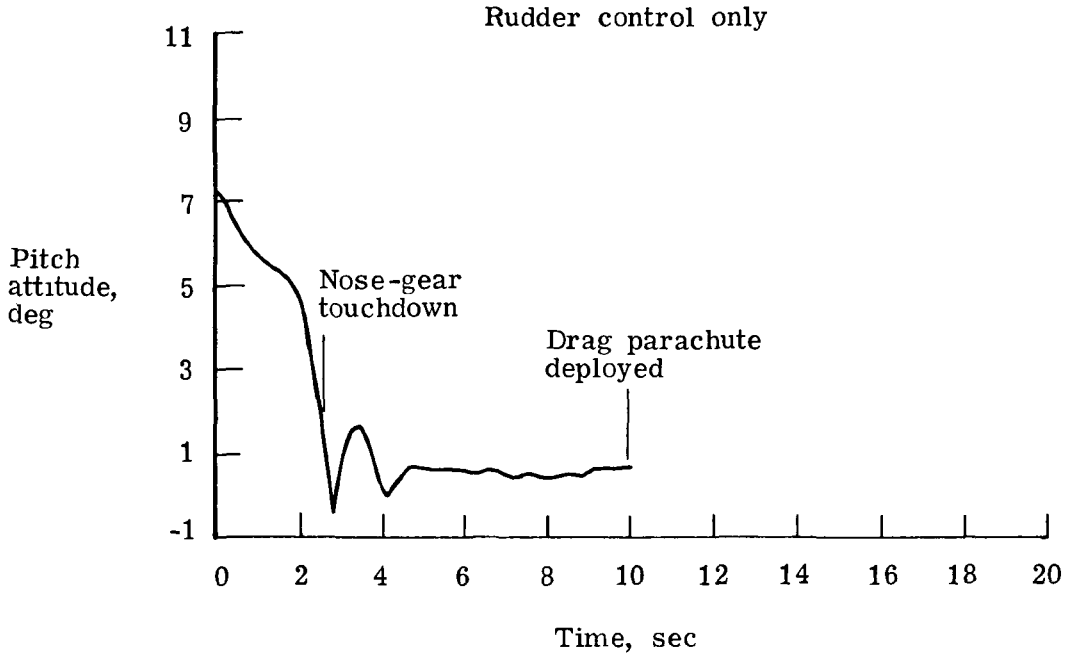

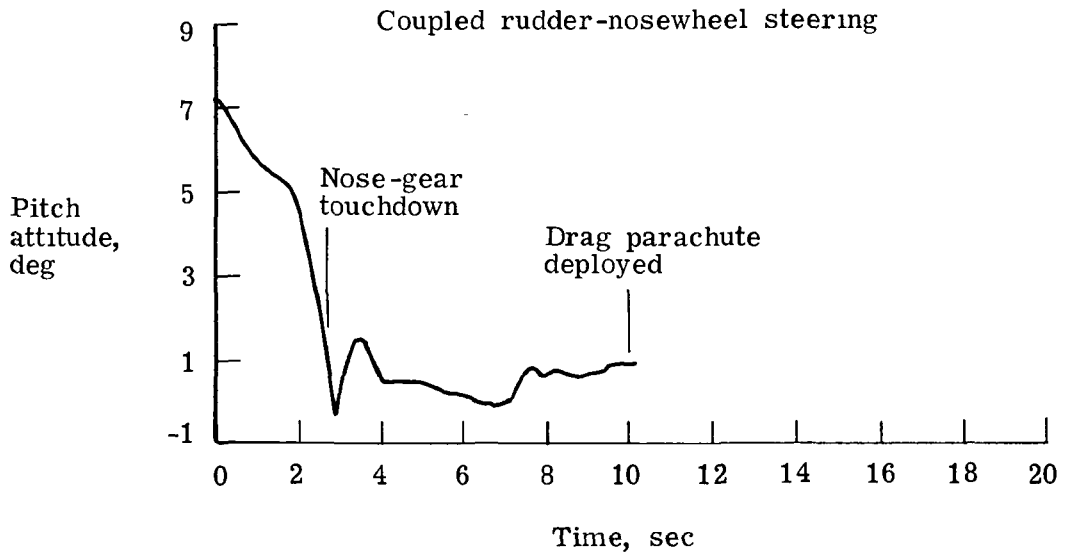

(d) Pitch attitude.

Figure 3.- Continued.

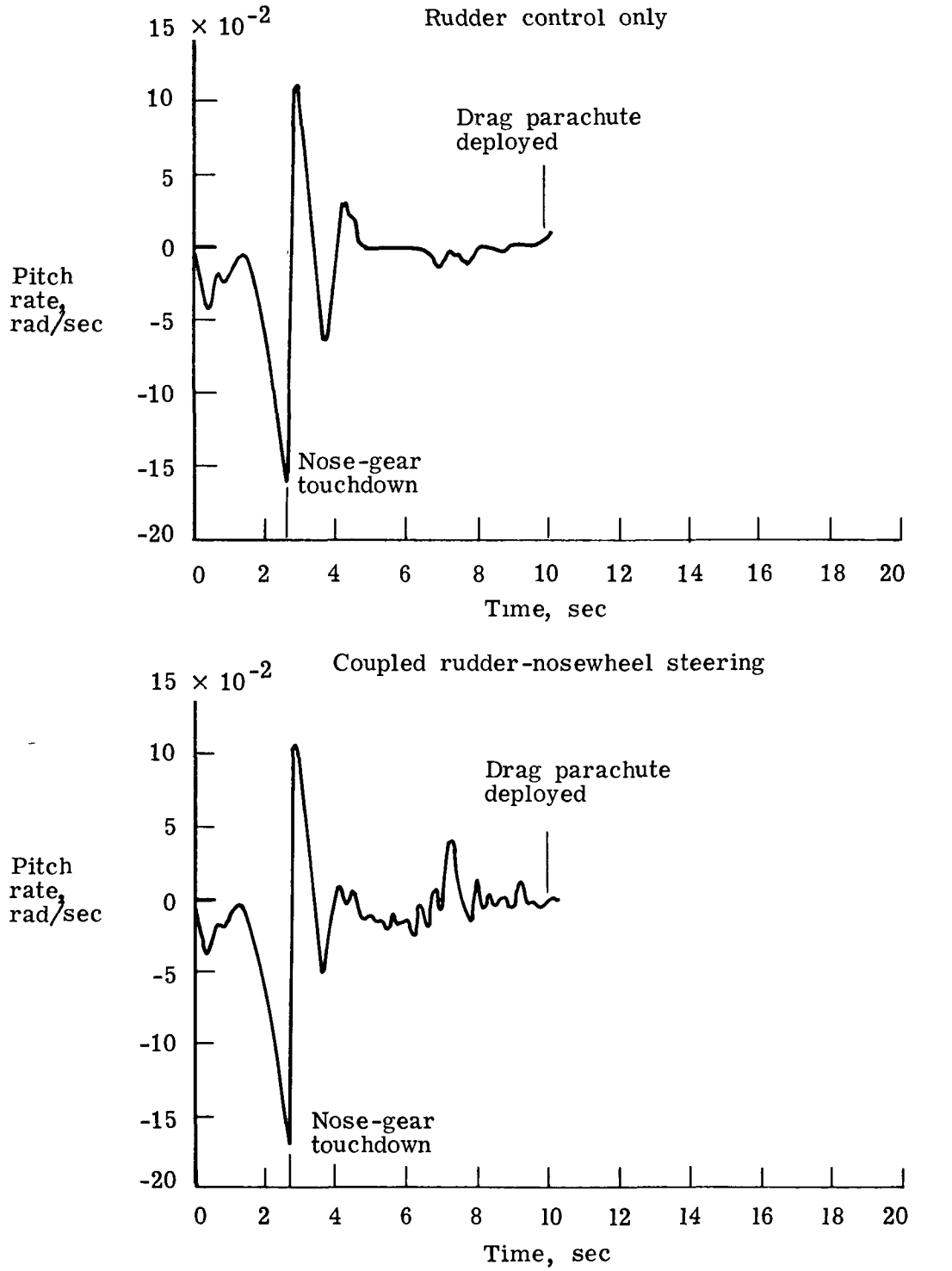

(e) Pitch rate.

Figure 3.- Continued.

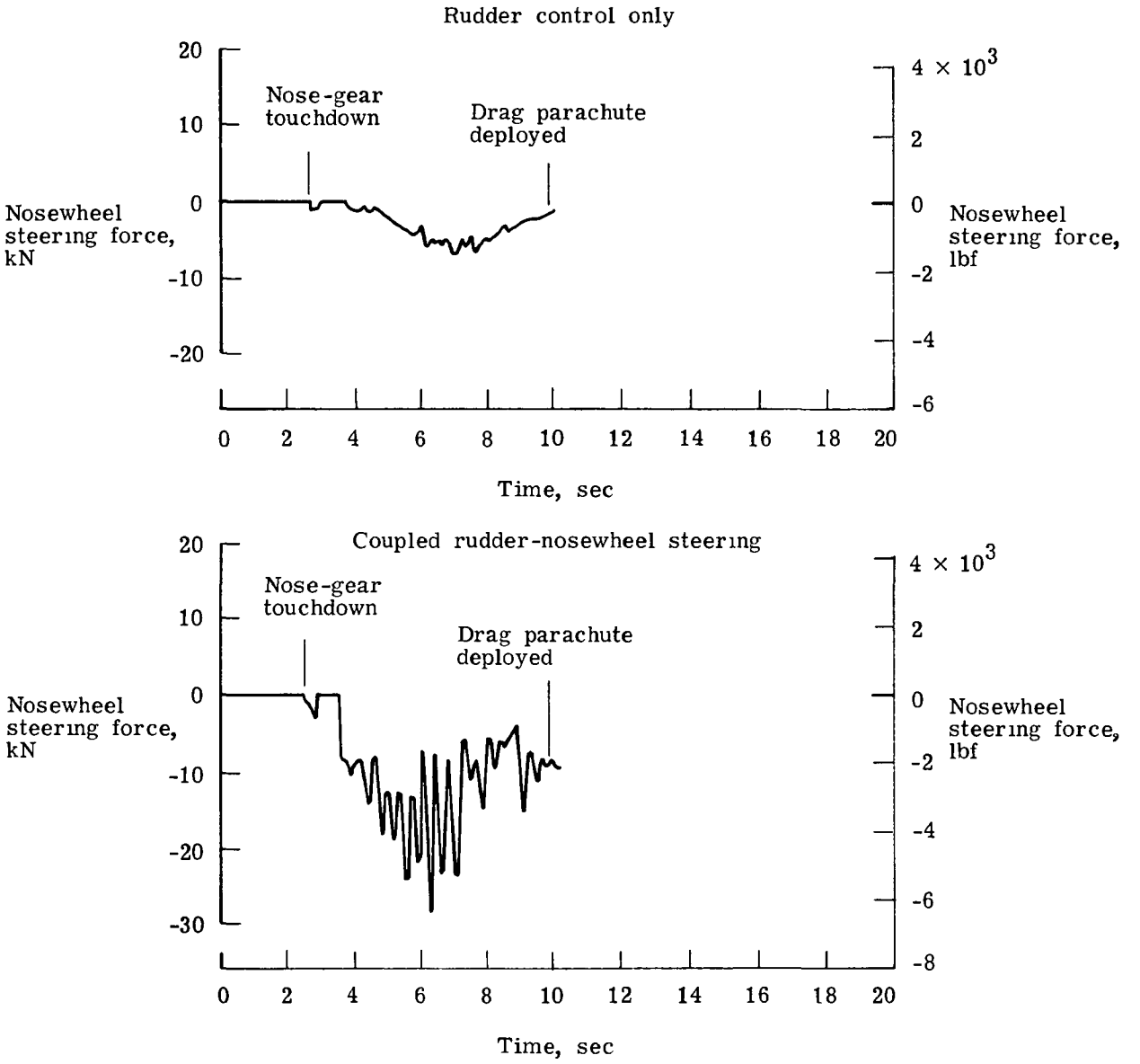

(f) Nosewheel steering force.

Figure 3.- Continued.

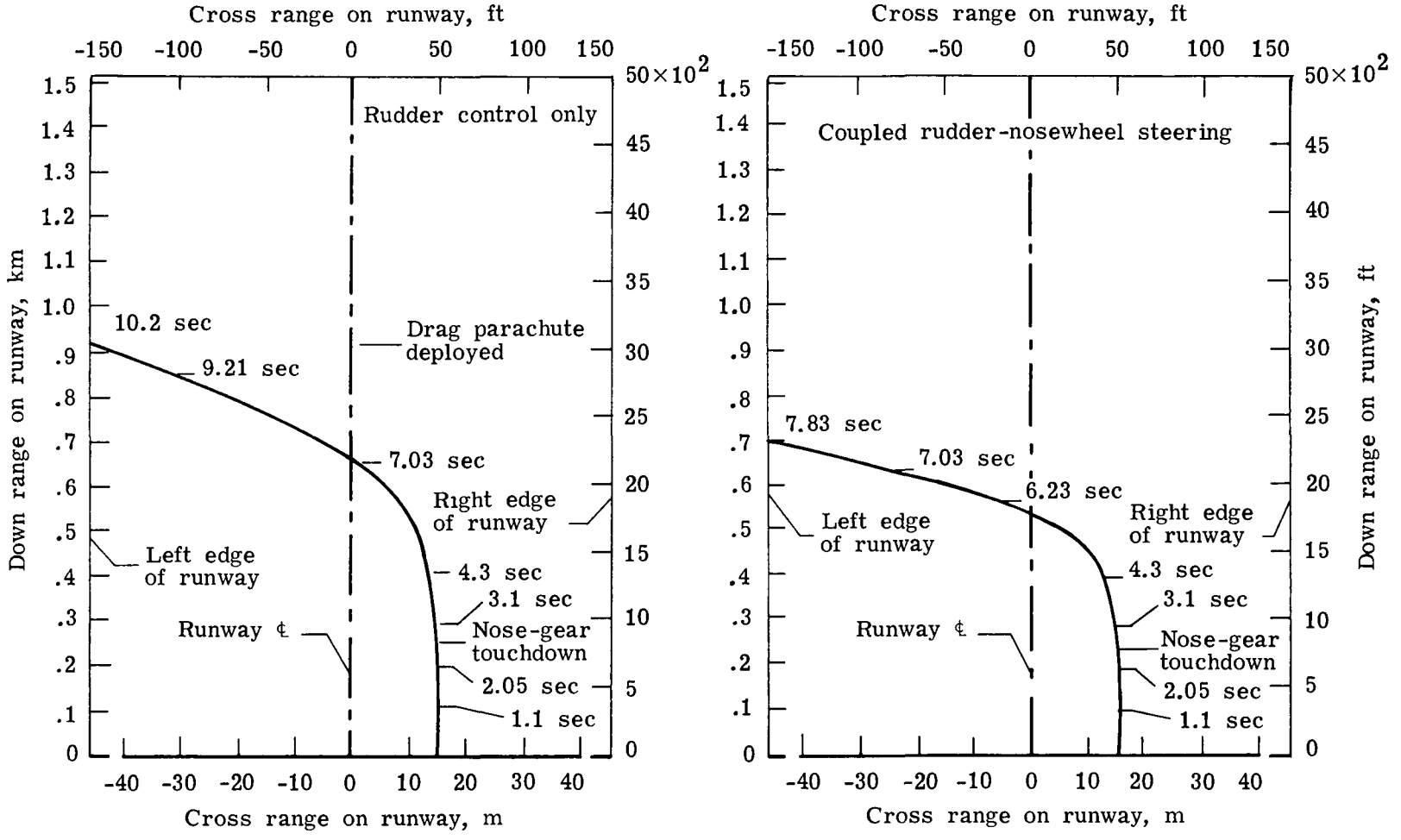

(g) Airplane c.g. position on runway.

Figure 3.- Continued.

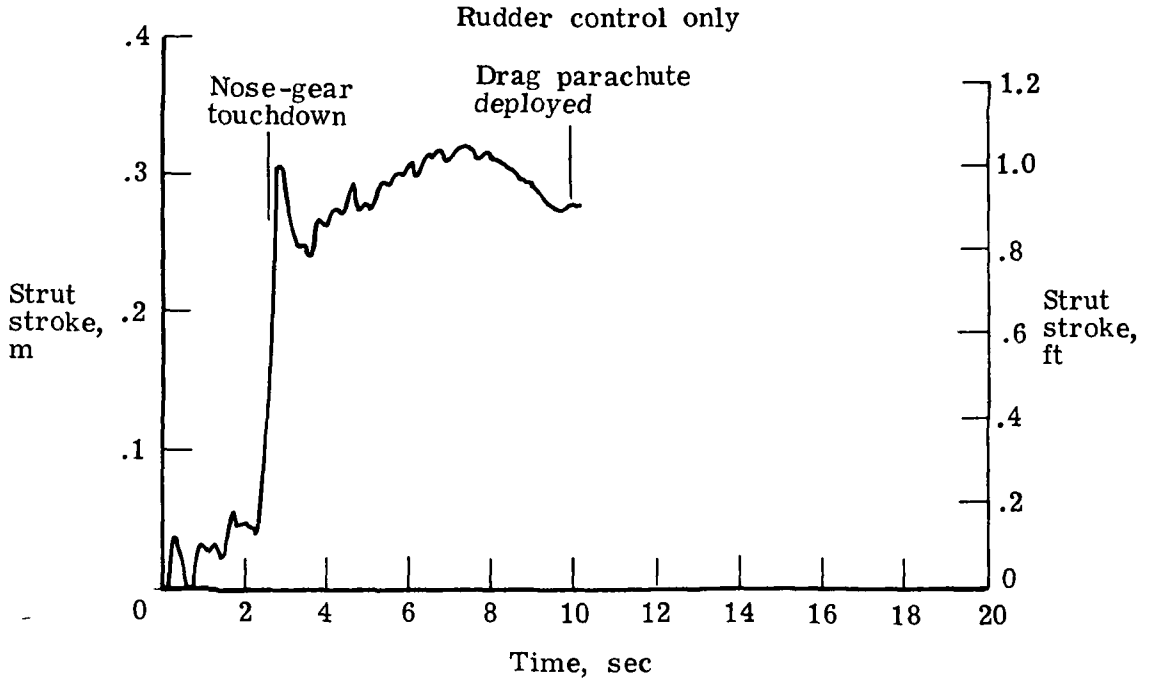

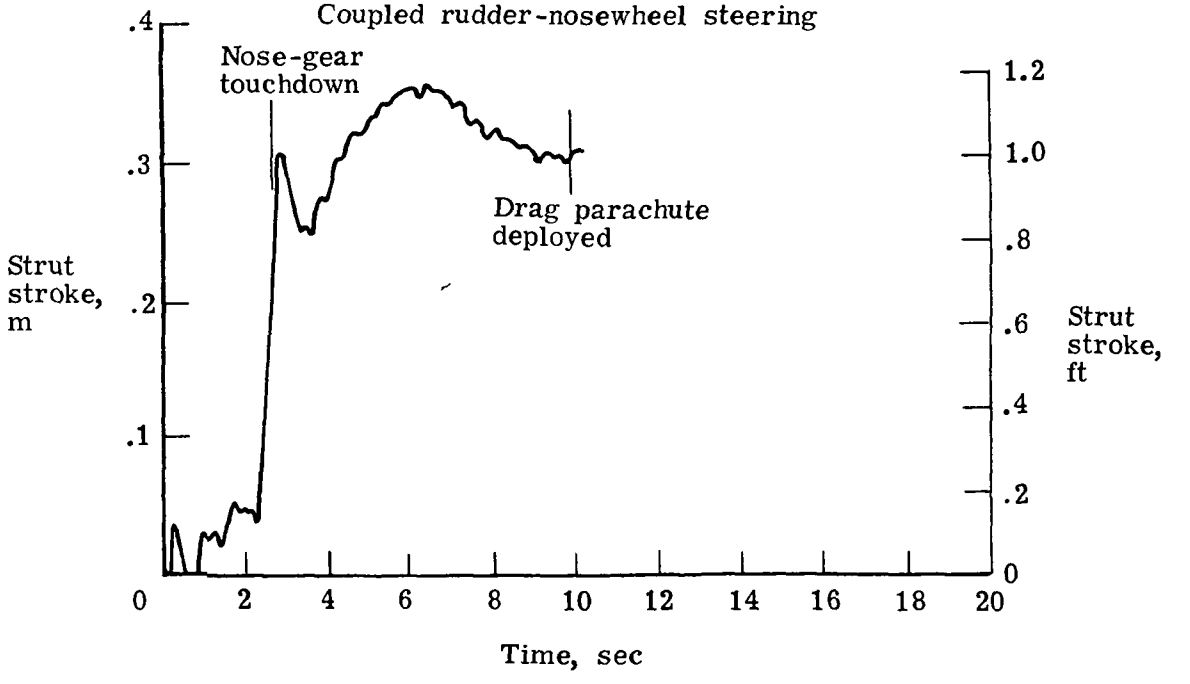

(h) Right-main-gear strut stroke.

Figure 3.- Continued.

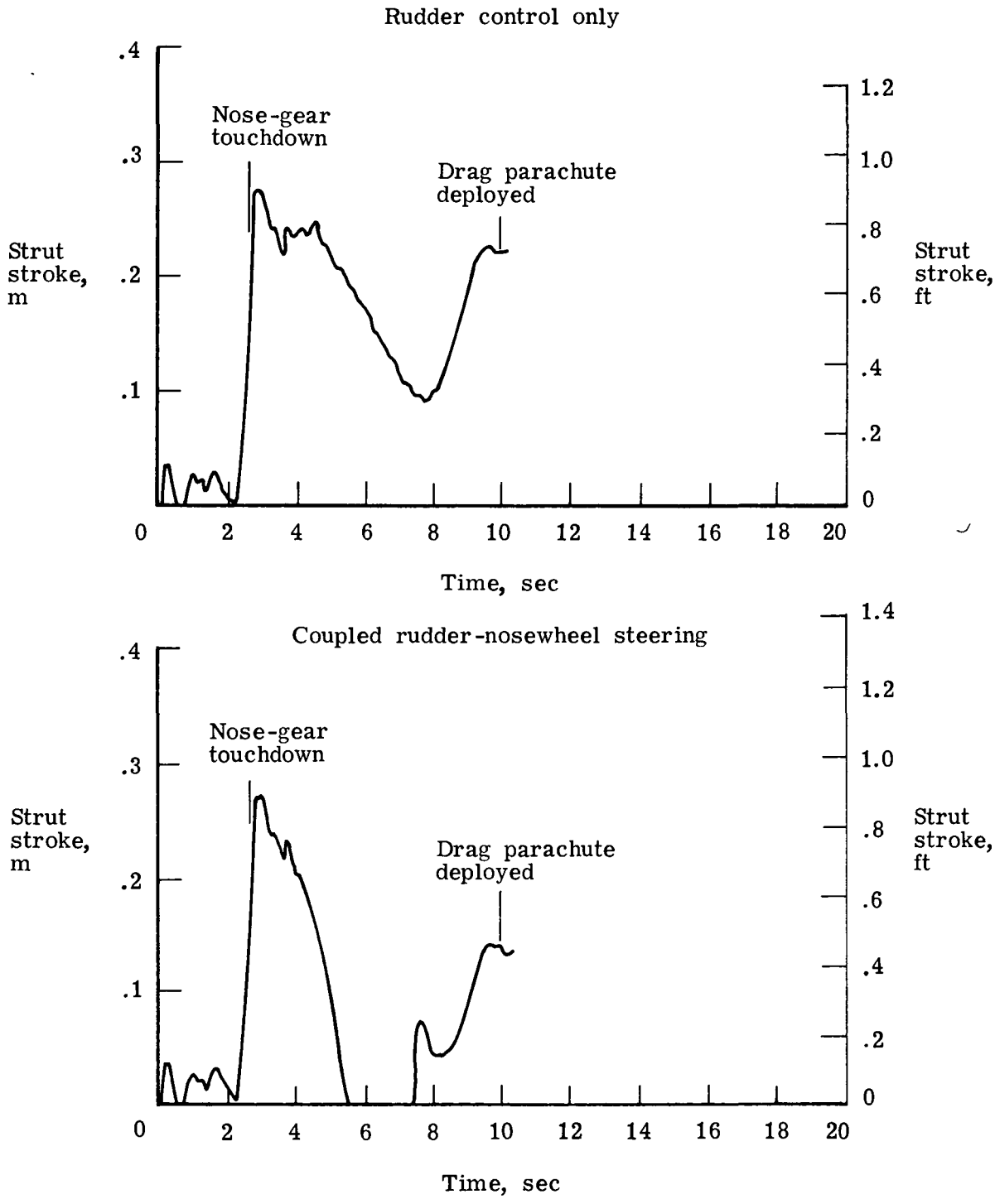

(i) Left-main-gear strut stroke.

Figure 3.- Continued.

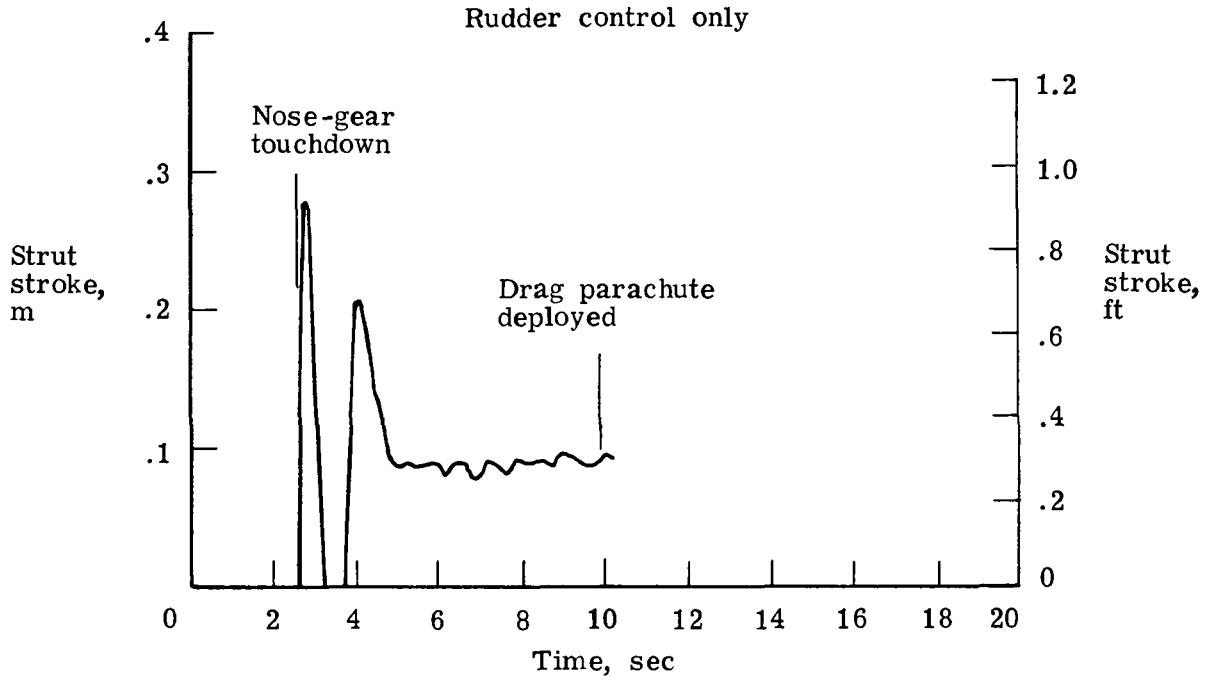

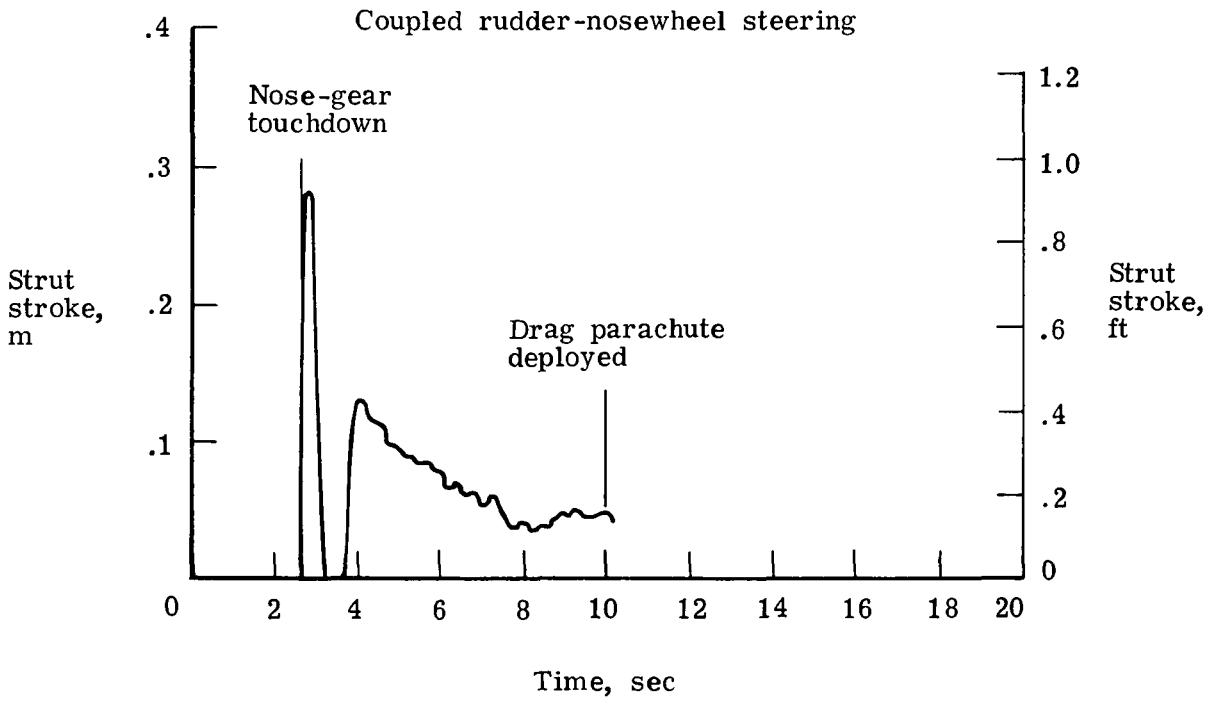

(j) Nose-gear strut stroke.

Figure 3.- Continued.

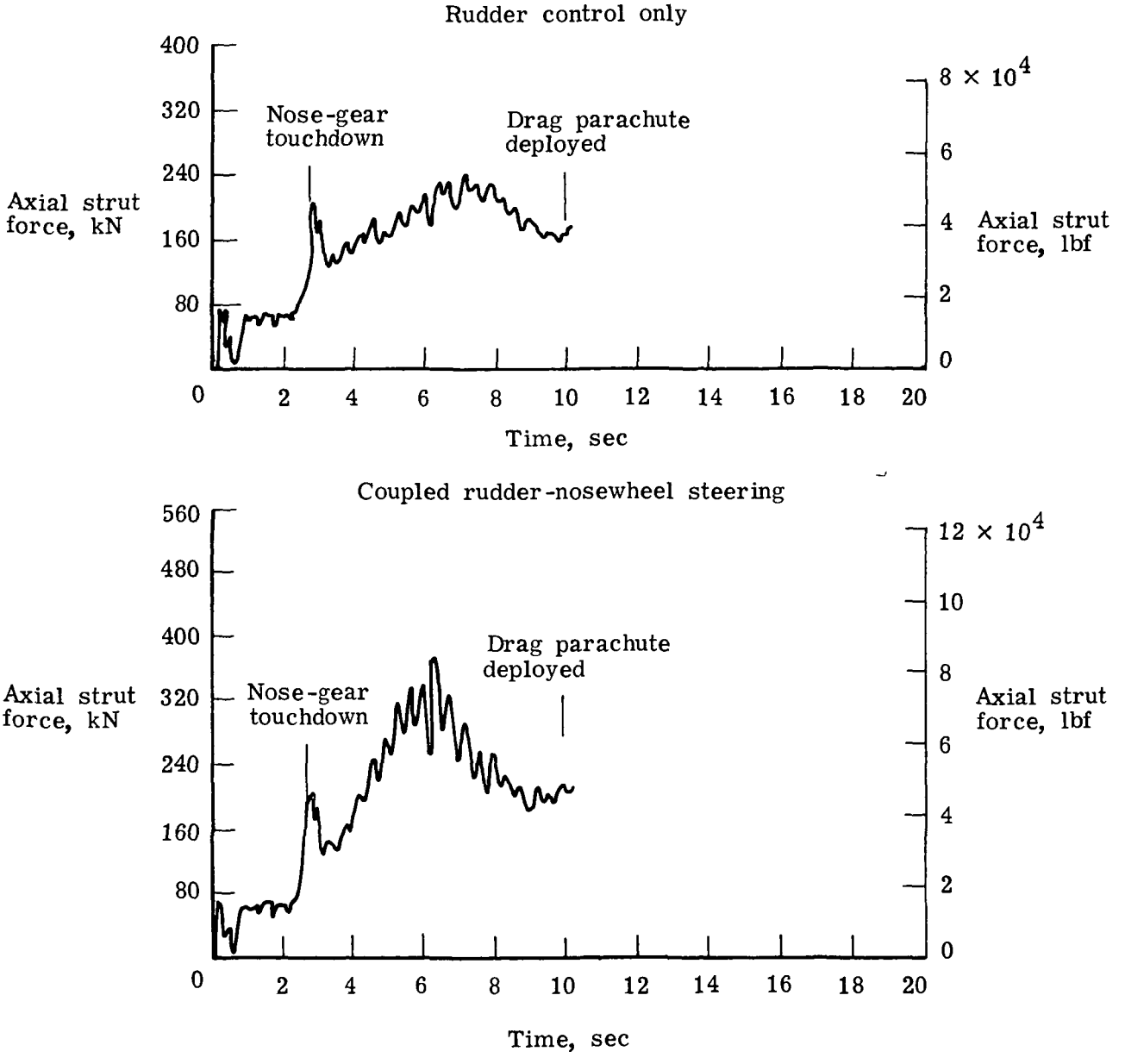

(k) Right-main-gear axial strut force.

Figure 3.- Continued.

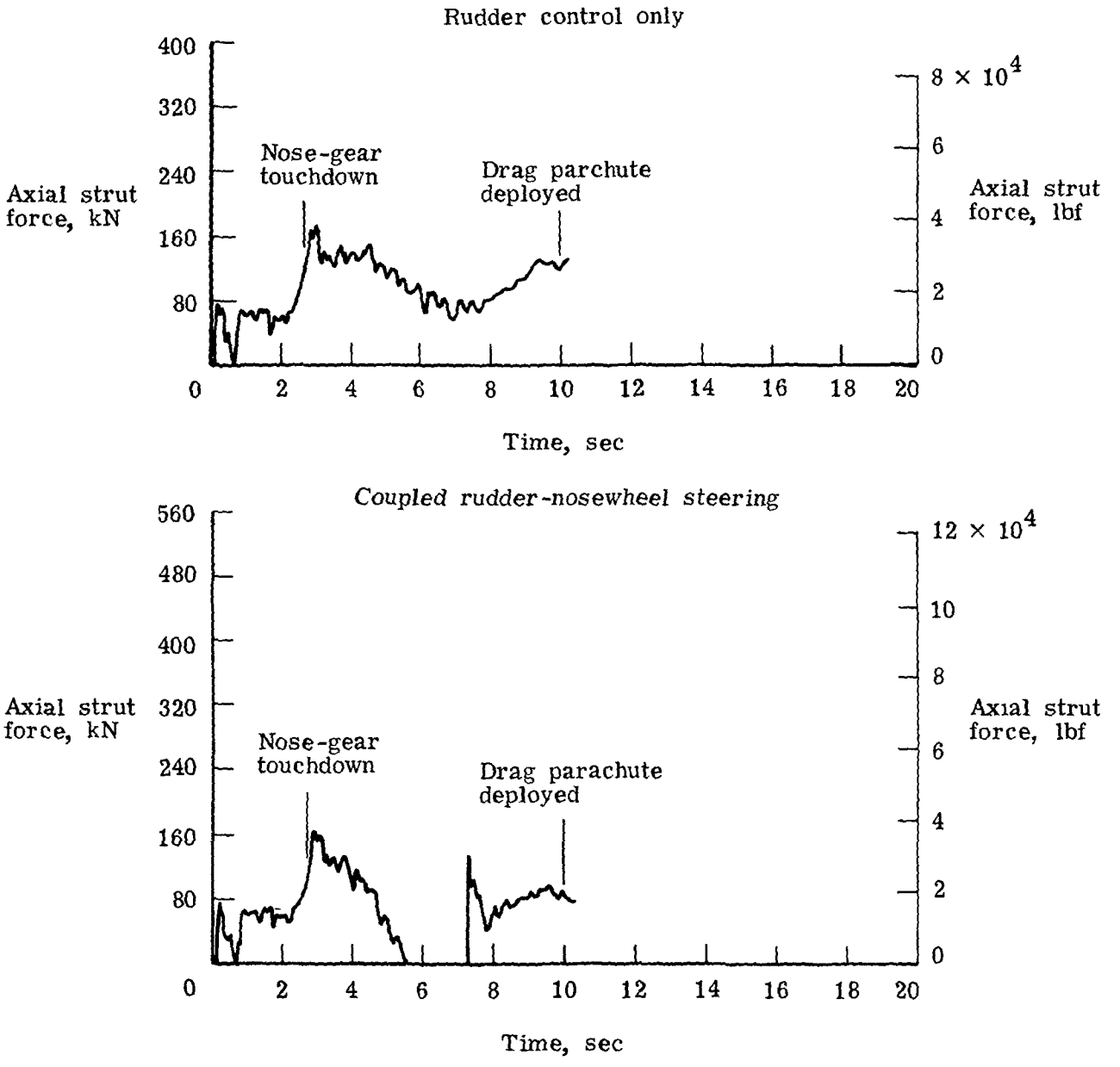

(1) Left-main-gear axial strut force.

Figure 3.- Continued.

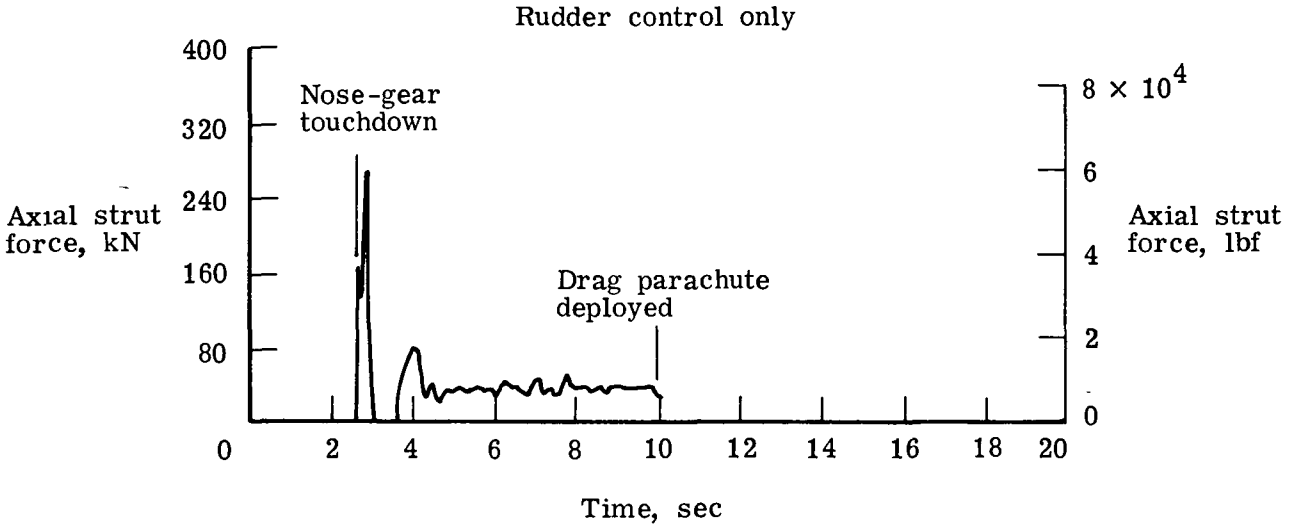

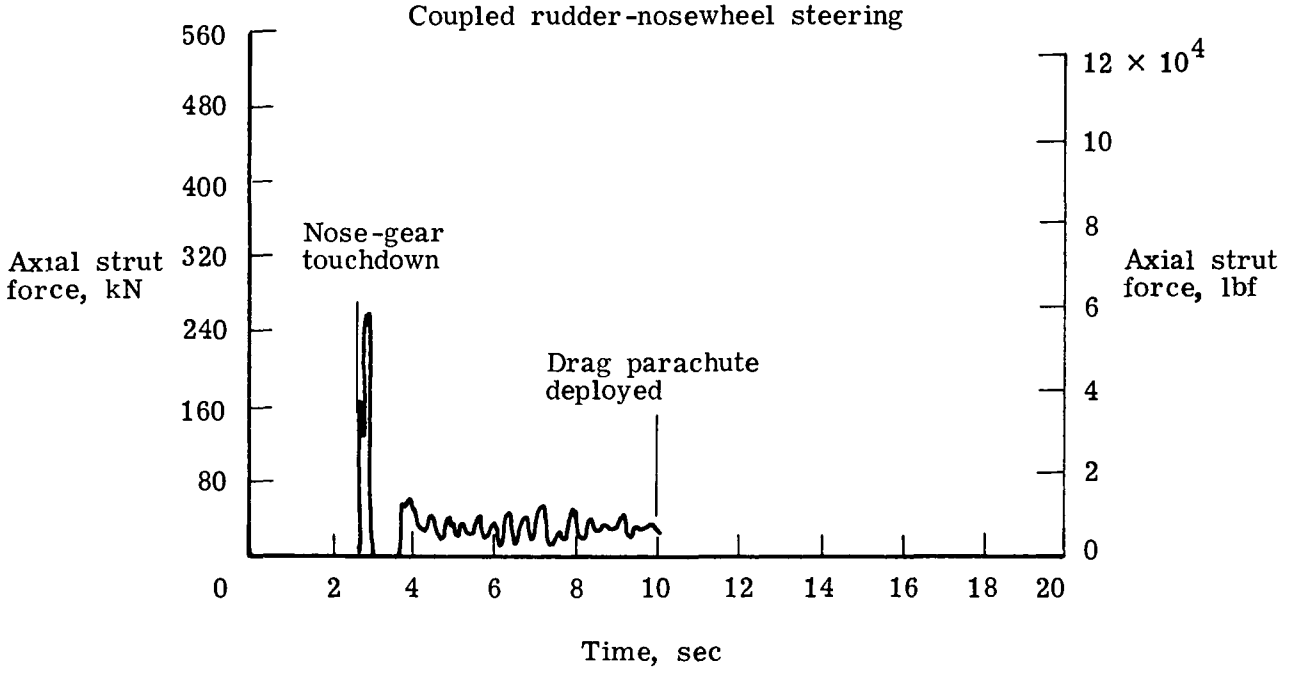

(m) Nose-gear axial strut force.

Figure 3.- Concluded.

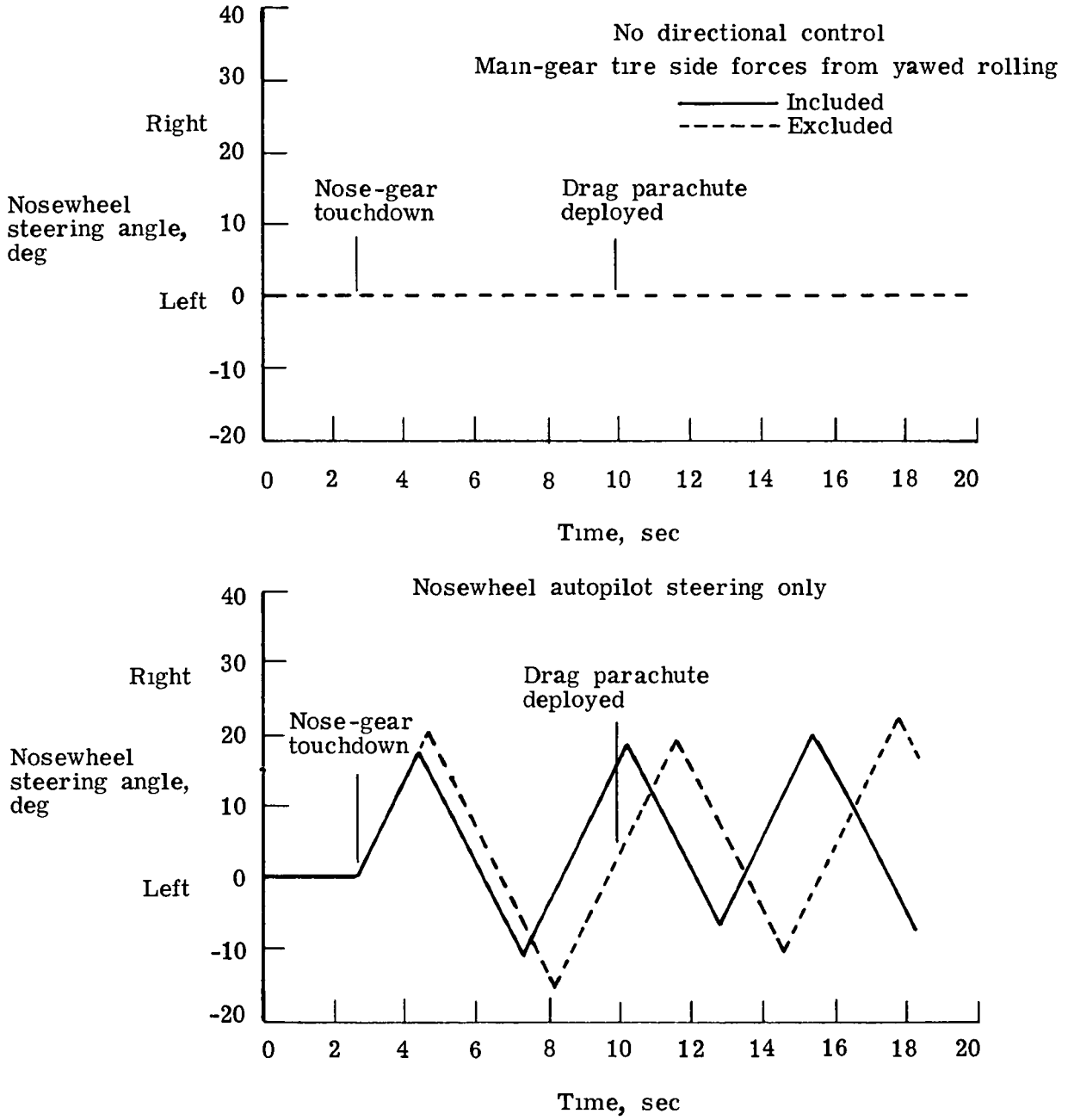

(a) Nosewheel steering angle.

Figure 4.- Analytical data for airplane crosswind landings with no directional control and with nosewheel autopilot steering only. Touchdown on runway center line. Wind velocity 7.62 m/sec (25 ft/sec).

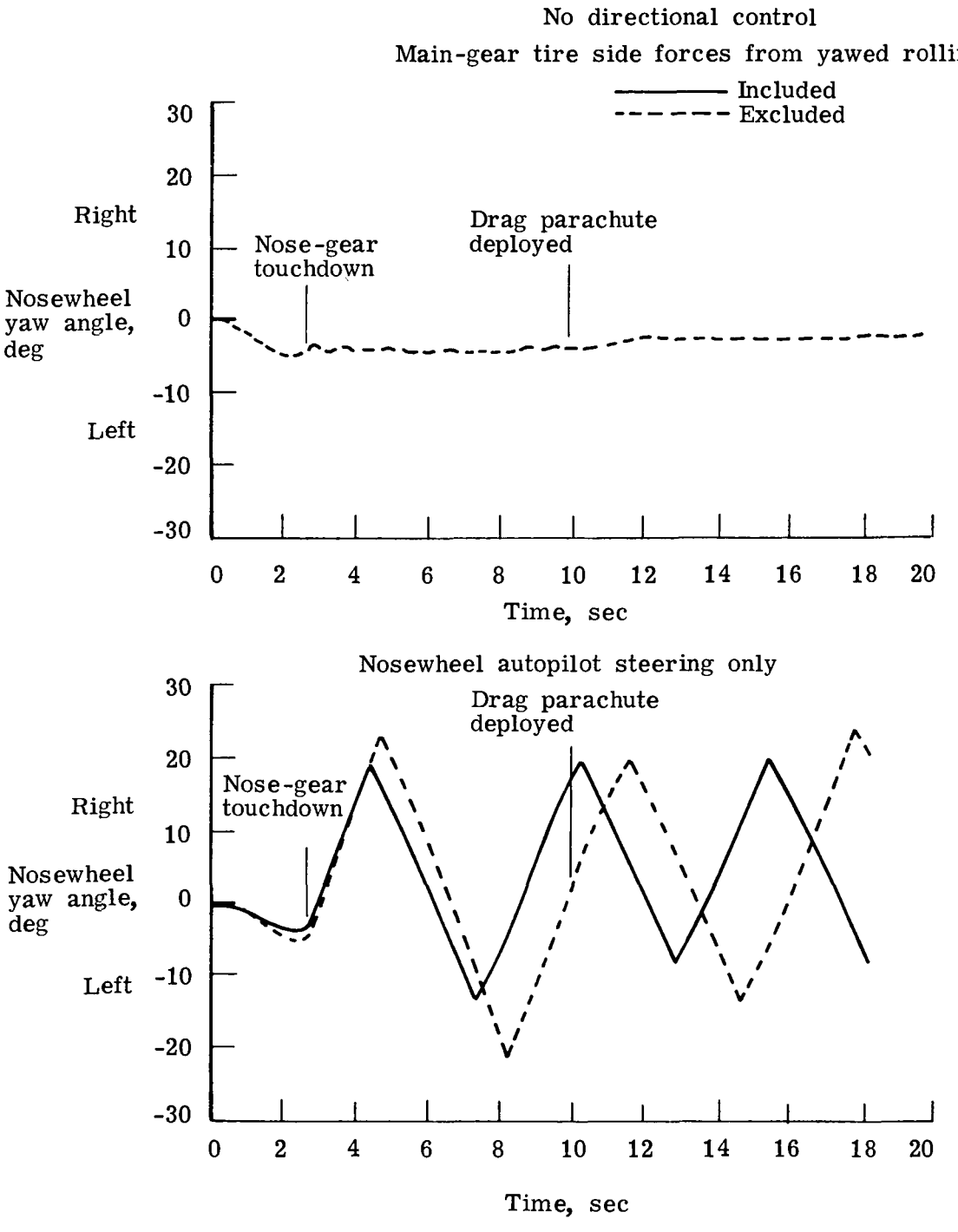

(b) Nosewheel yaw angle.

Figure 4.- Continued.

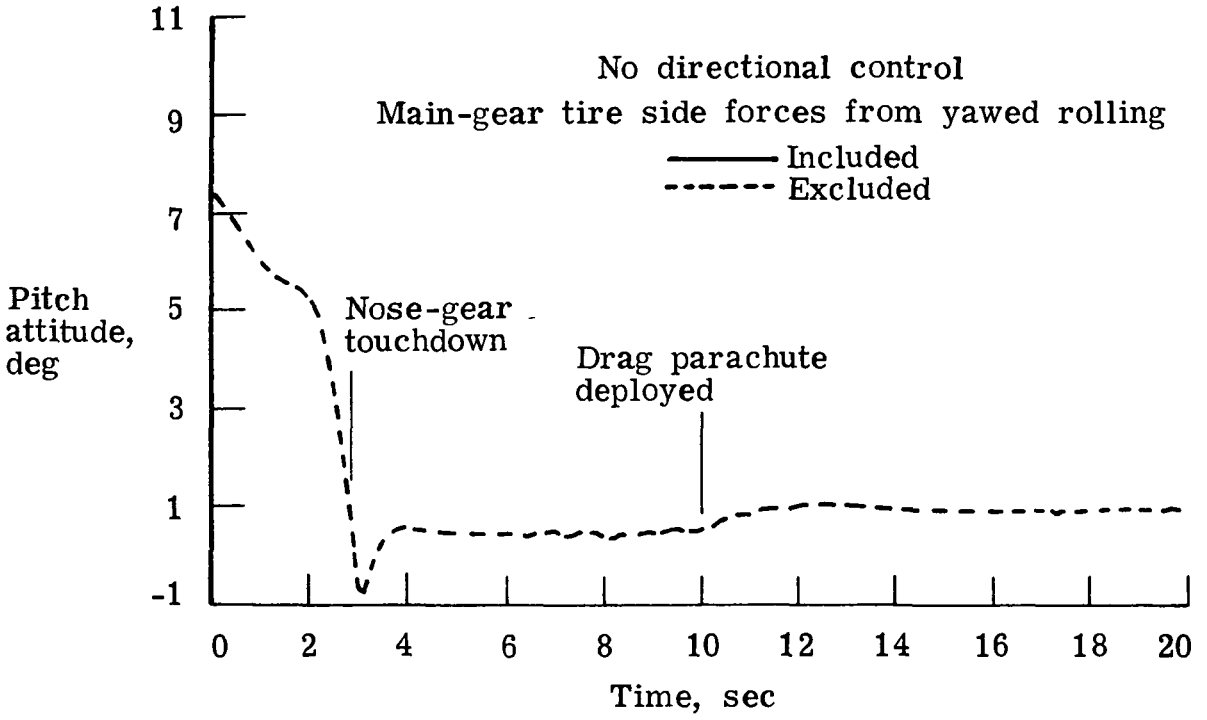

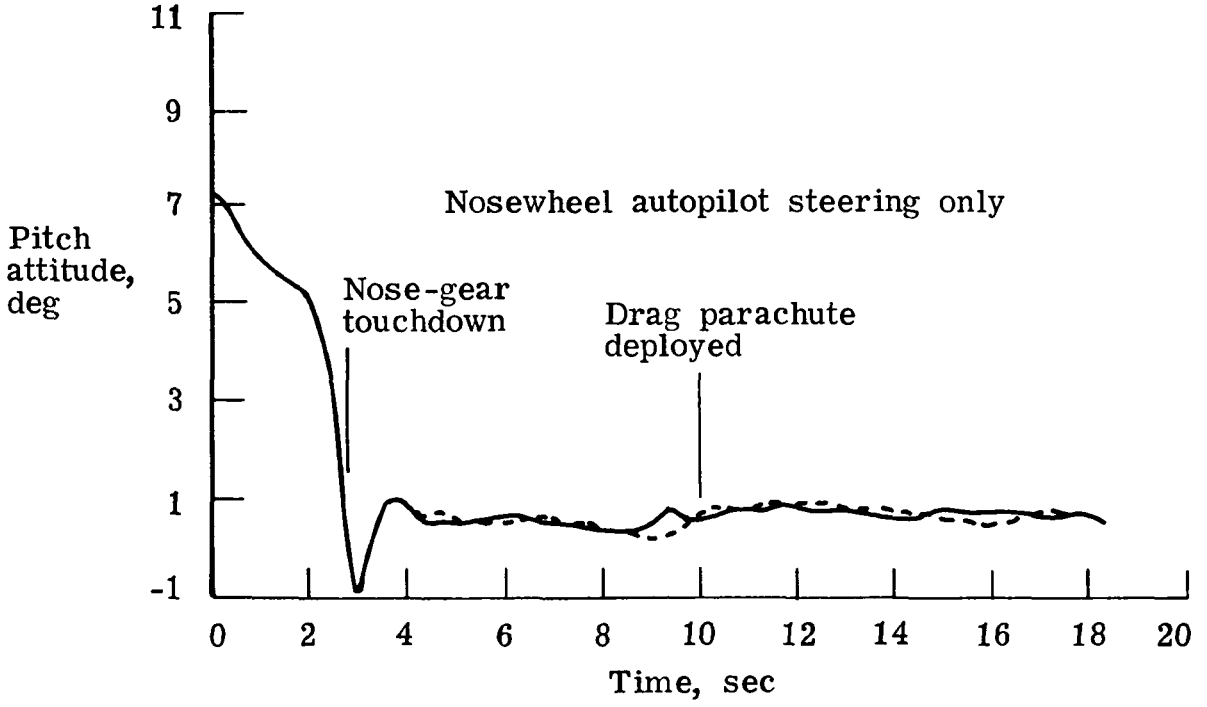

(c) Pitch attitude.

Figure 4.- Continued.

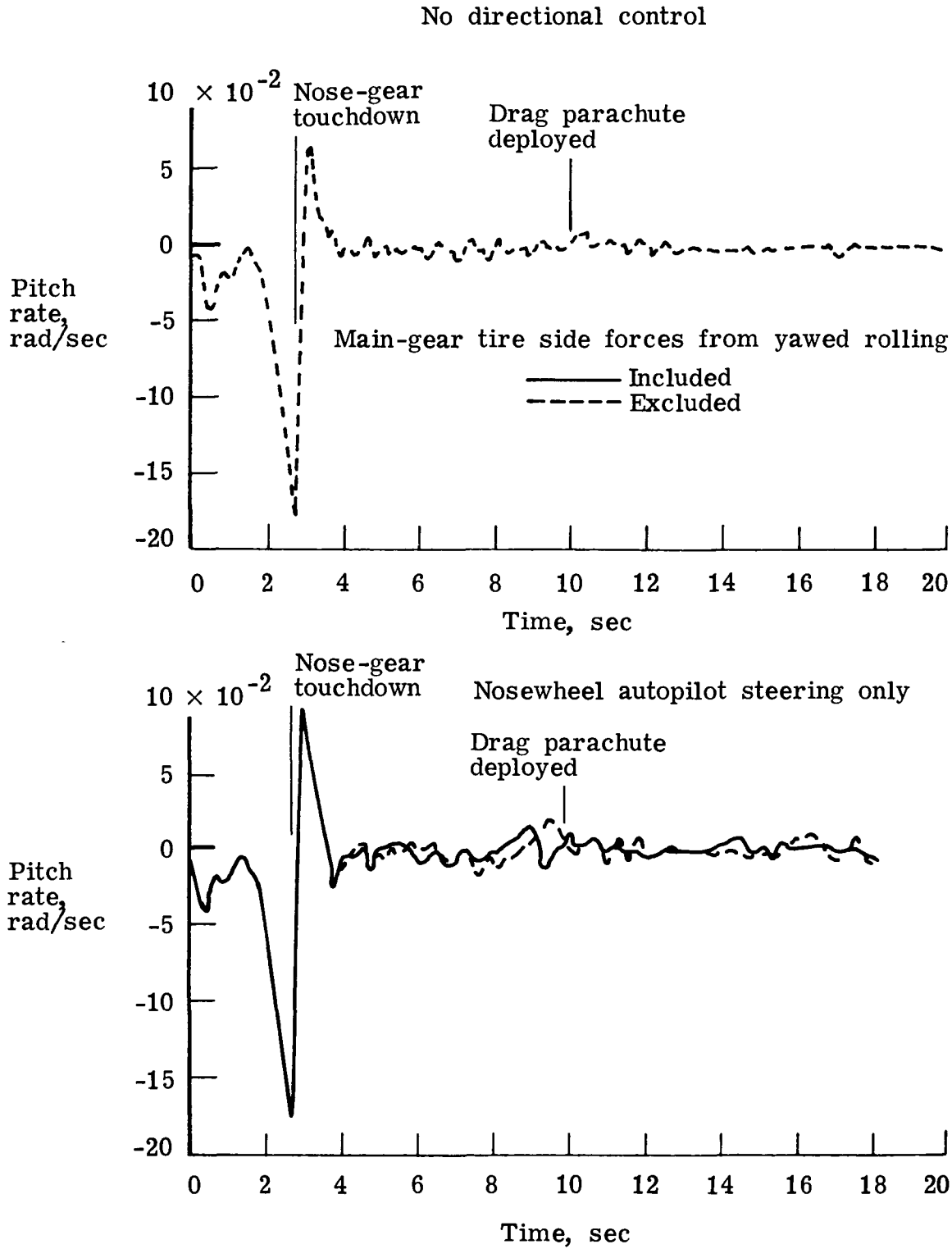

(d) Pitch rate.

Figure 4.- Continued.

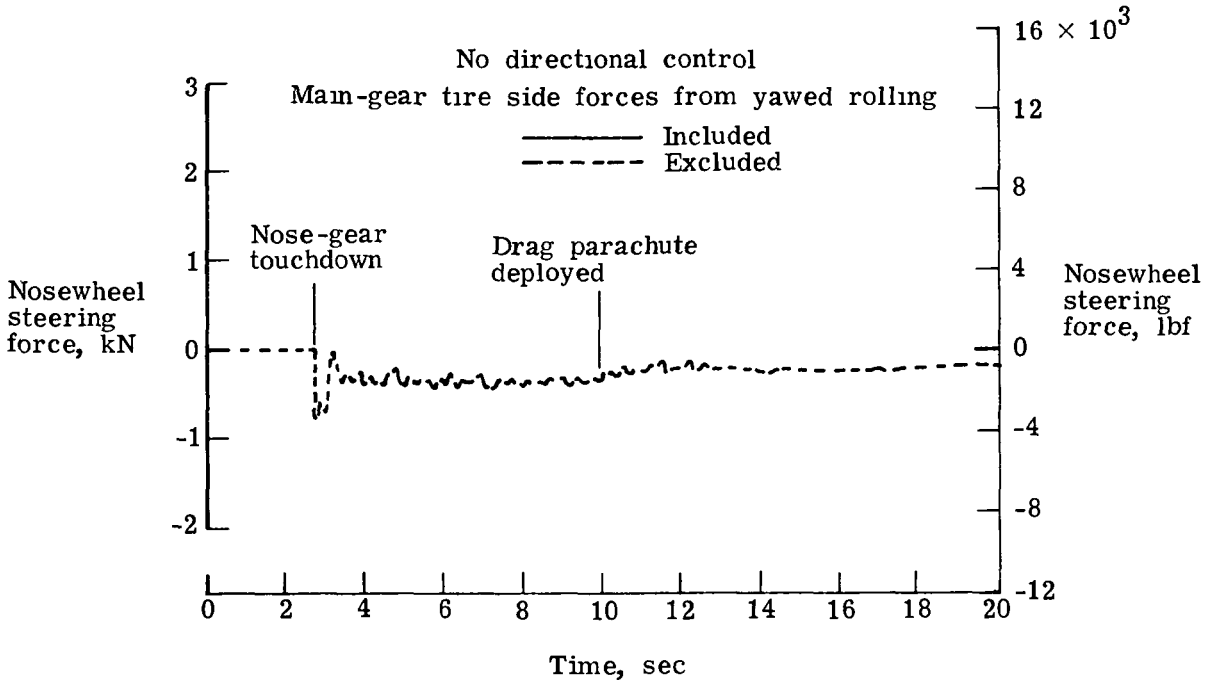

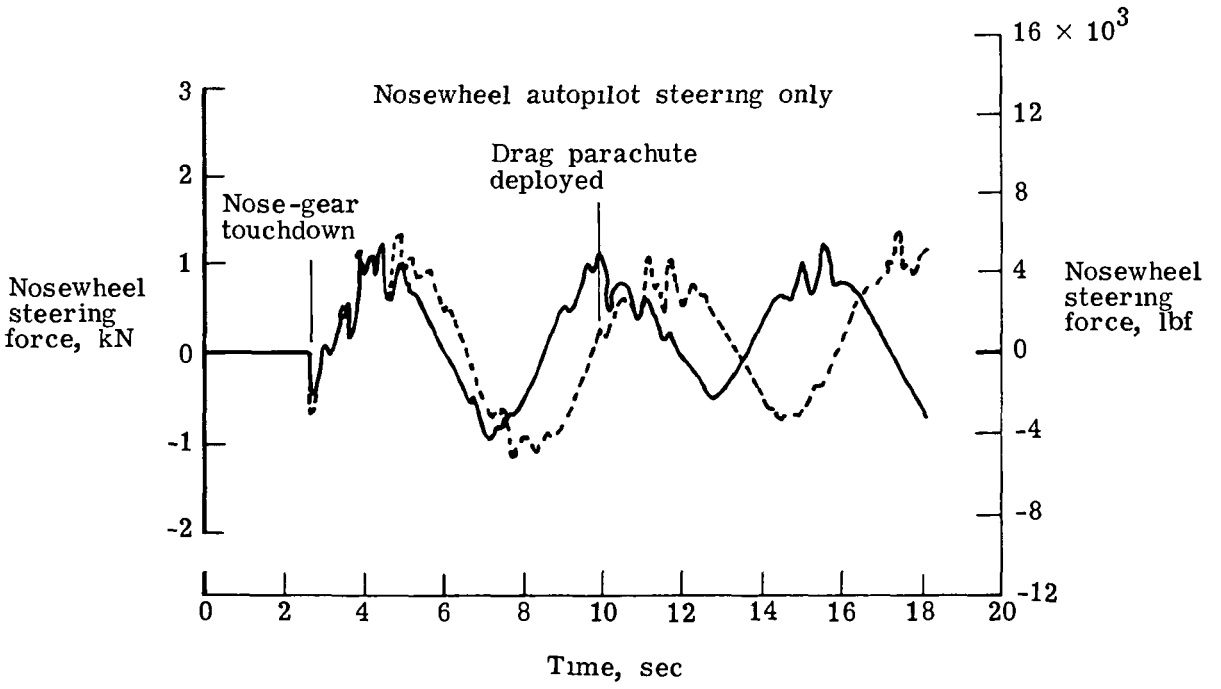

(e) Nosewheel steering force.

Figure 4.- Continued.

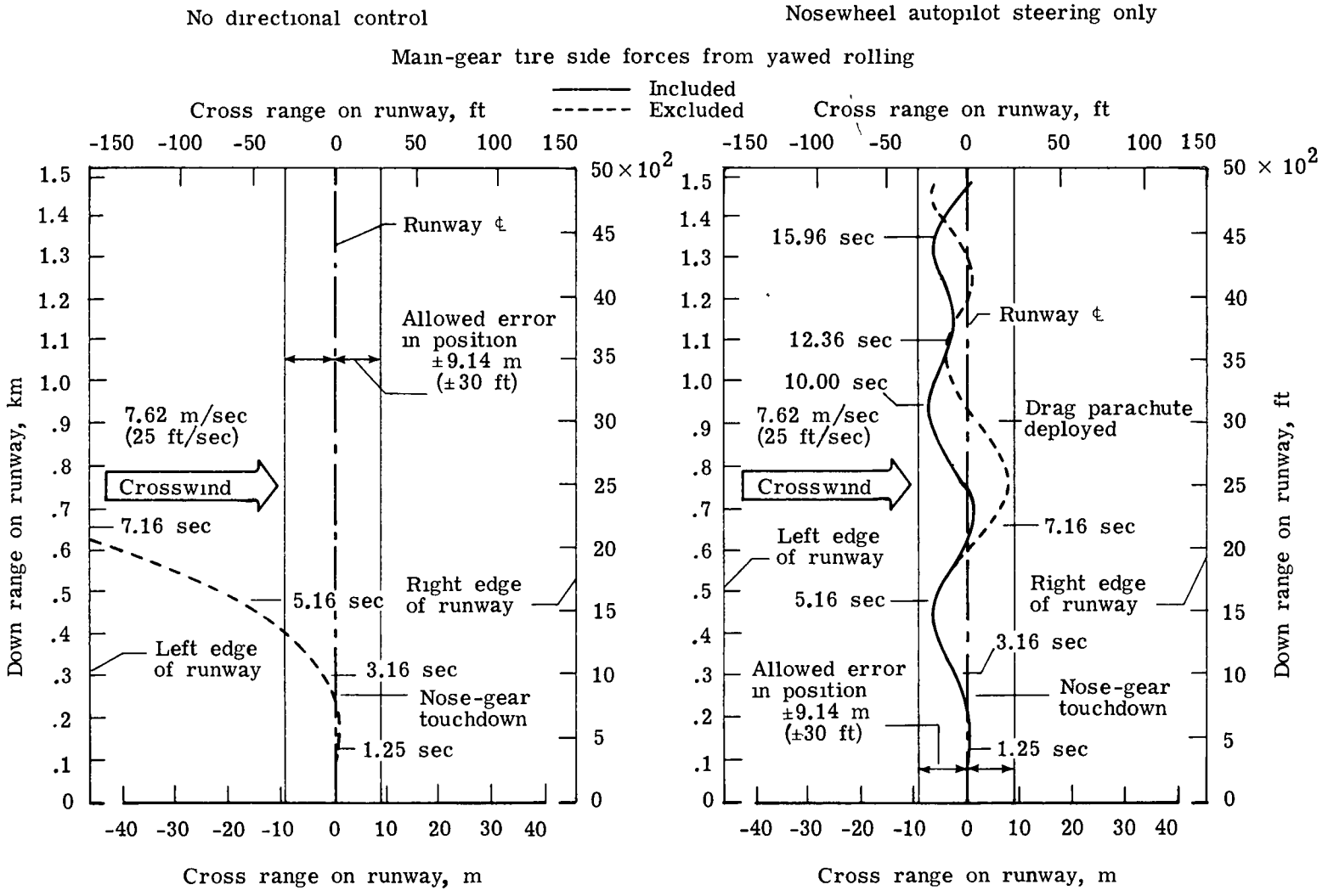

(f) Airplane c.g. position on runway.

Figure 4.- Continued.

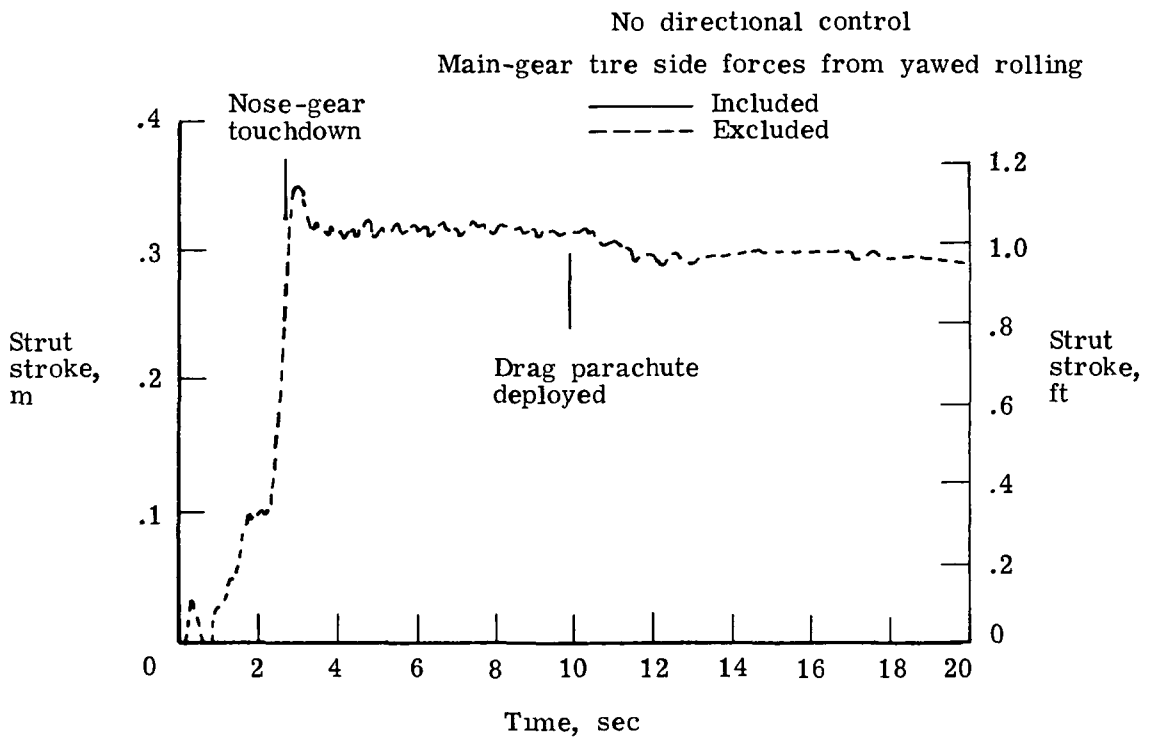

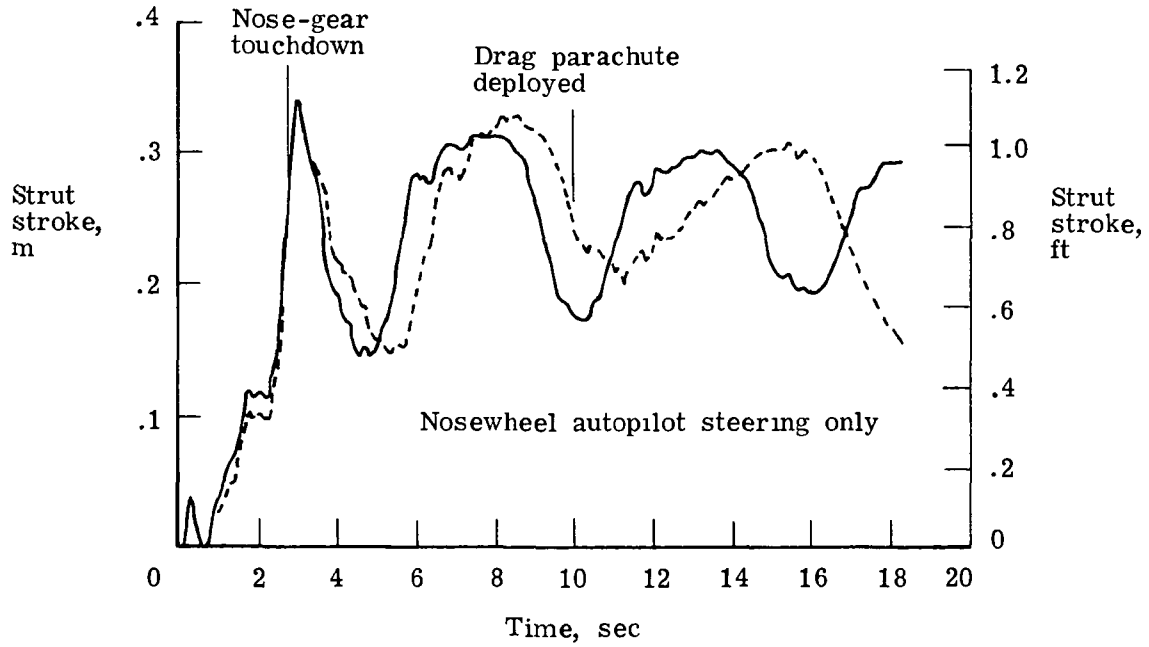

(g) Right-main-gear strut stroke.

Figure 4.- Continued.

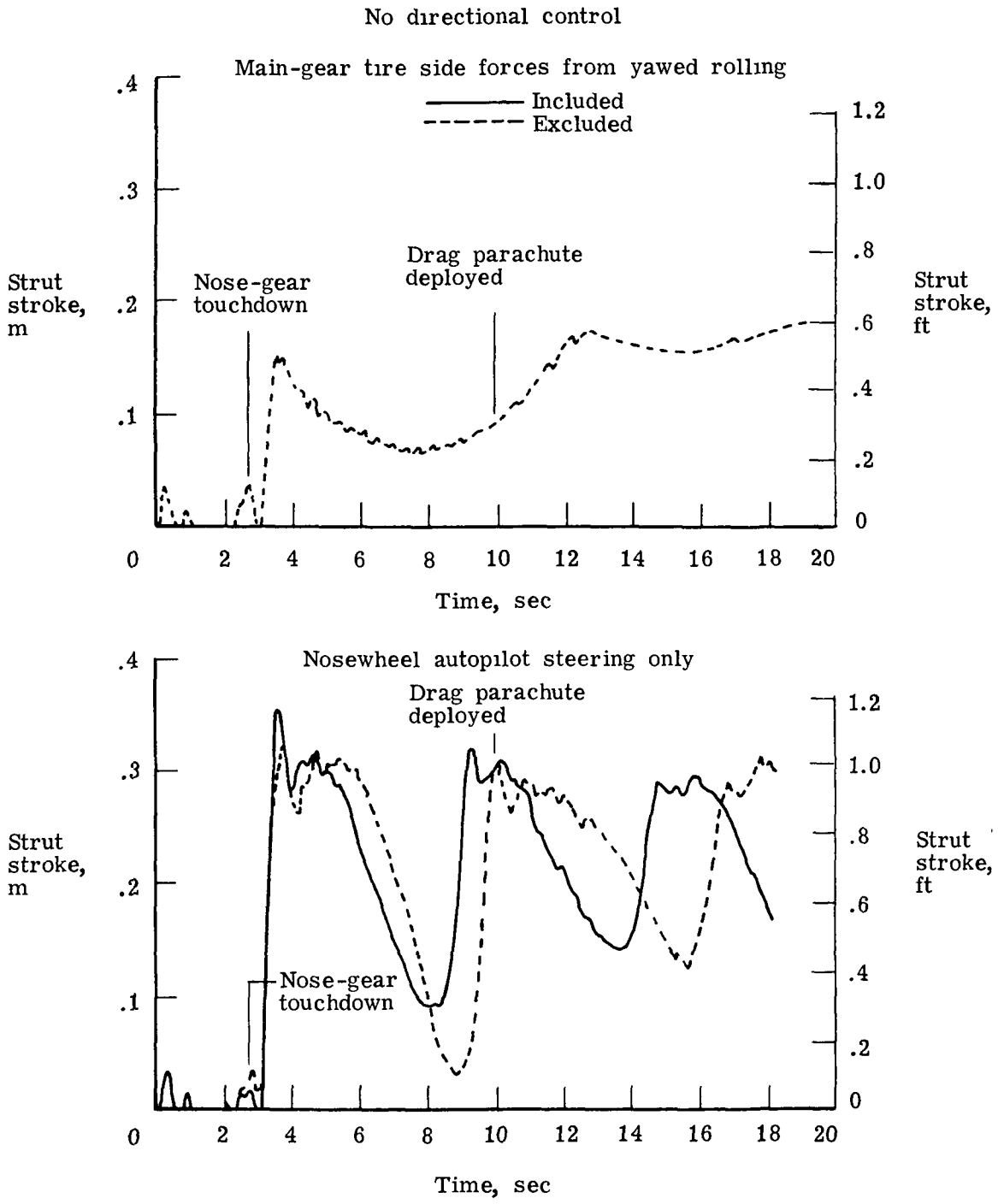

(h) Left-main-gear strut stroke.

Figure 4.- Continued.

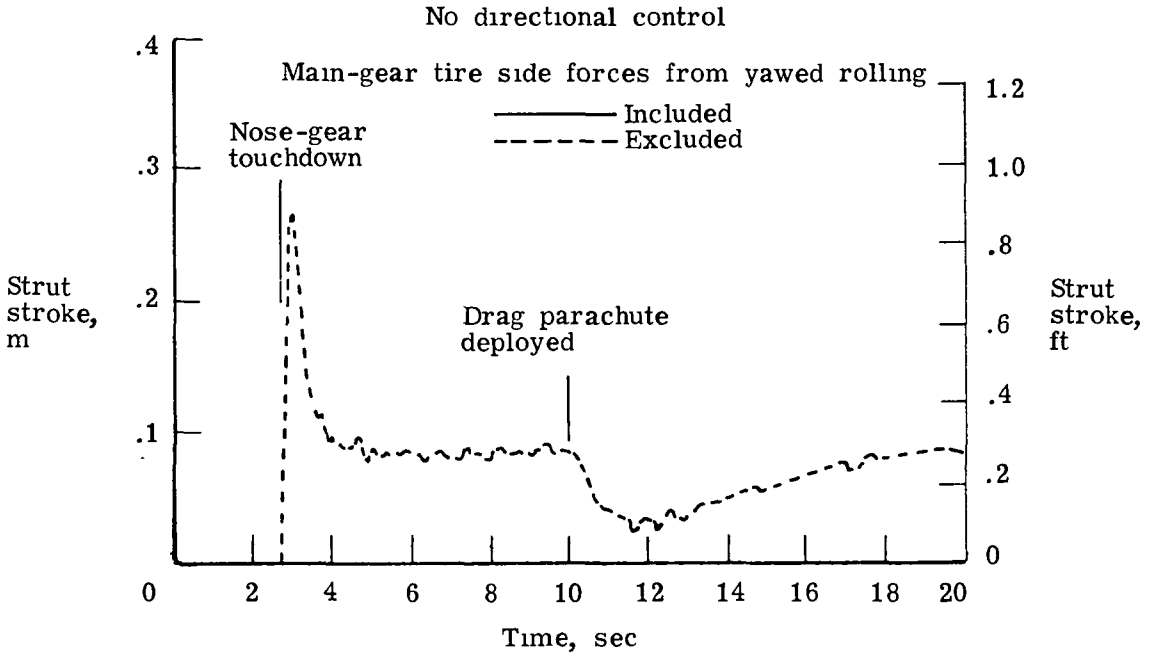

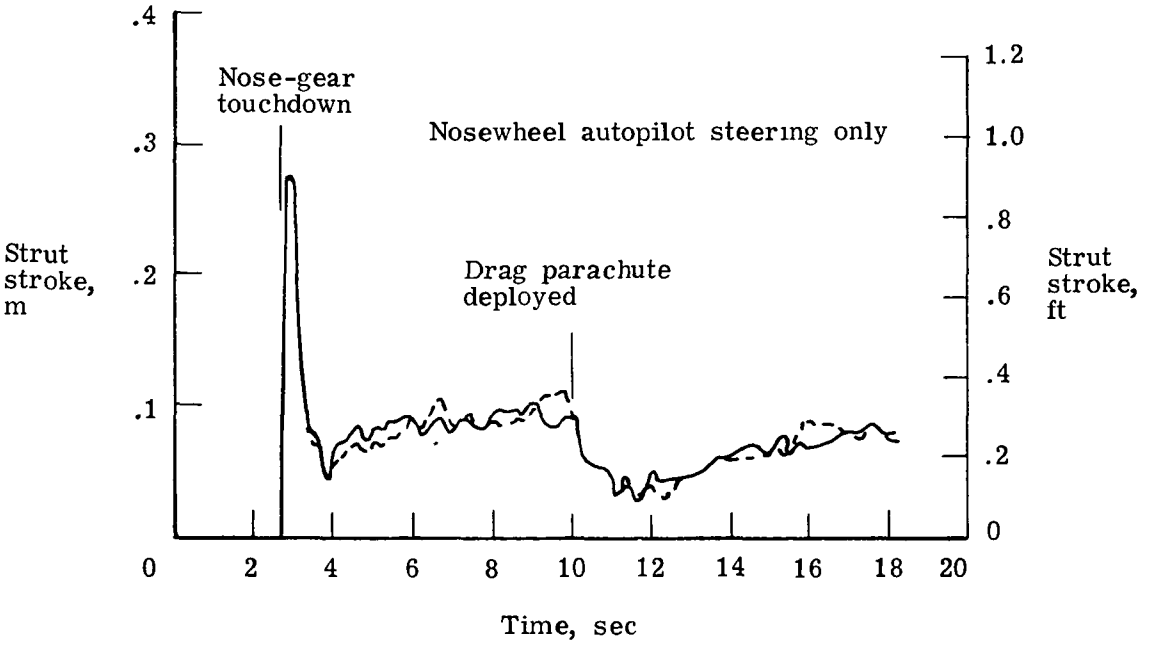

(i) Nose-gear strut stroke.

Figure 4.- Continued.

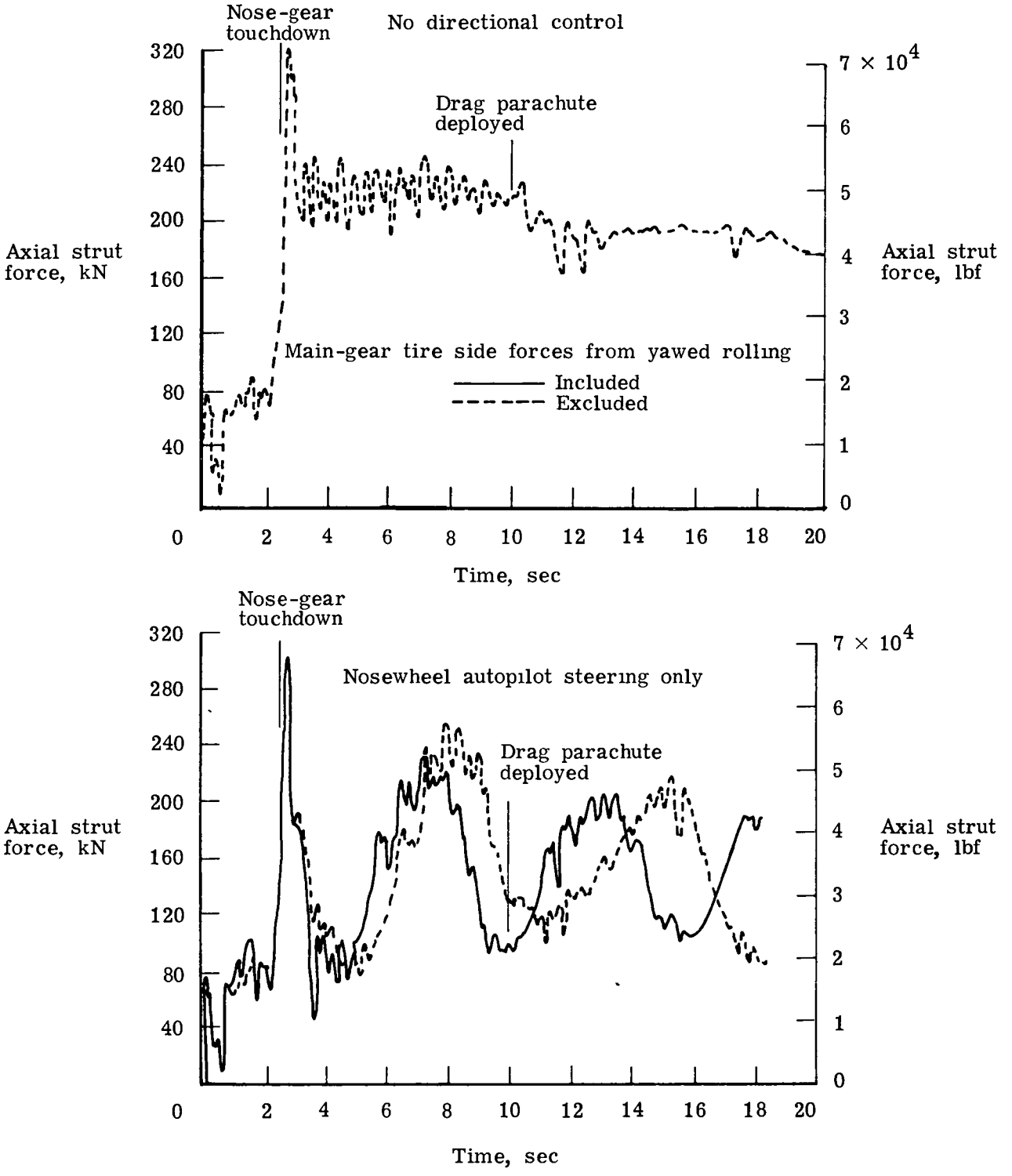

(j) Right-main-gear axial strut force.

Figure 4.- Continued.

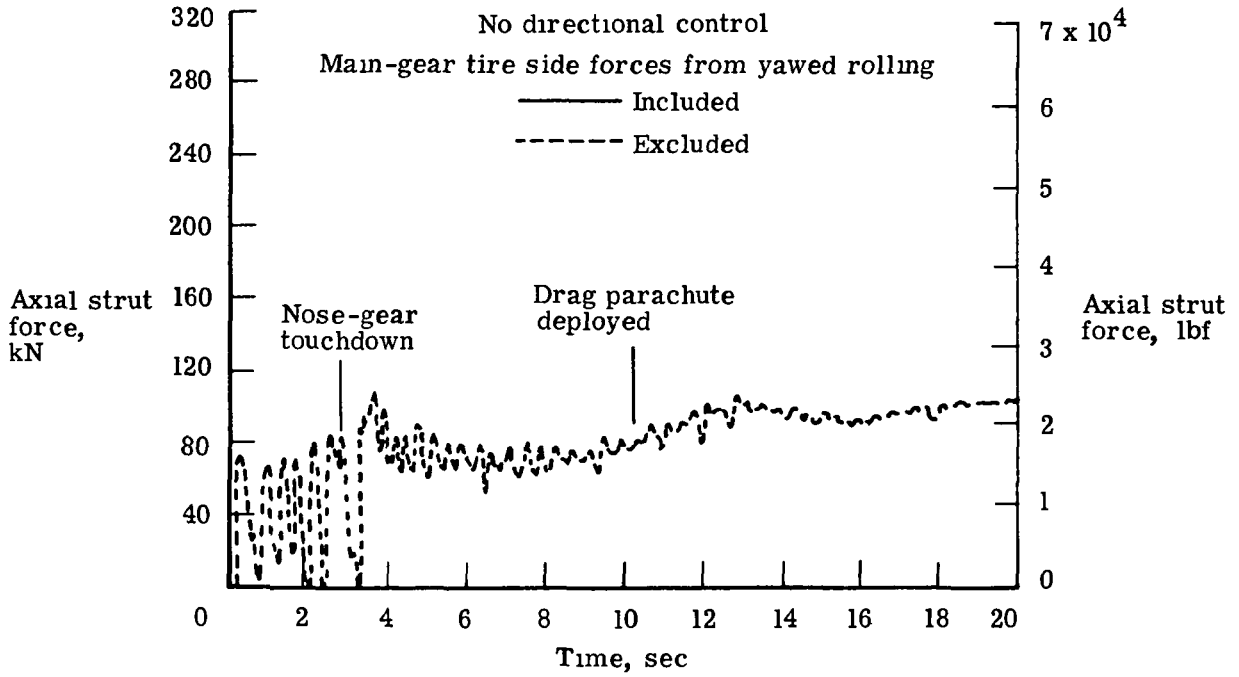

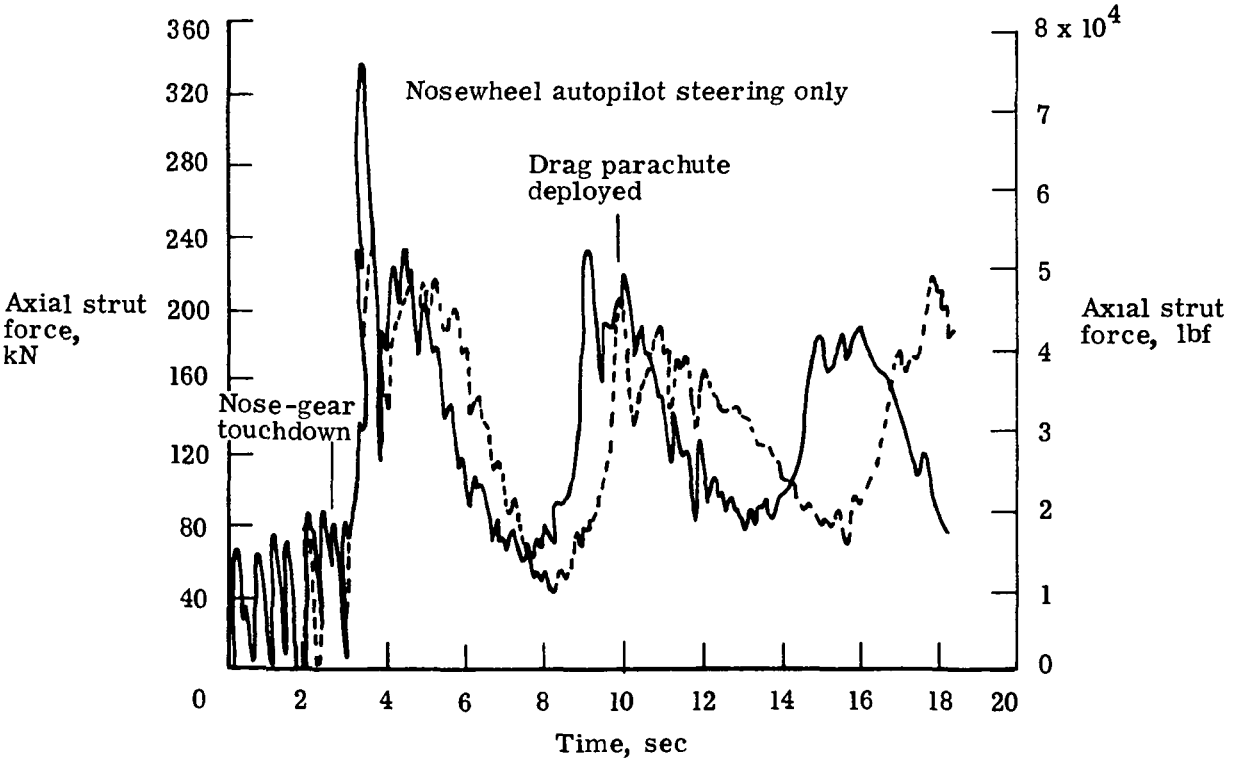

(k) Left-main-gear axial strut force.

Figure 4.- Continued.

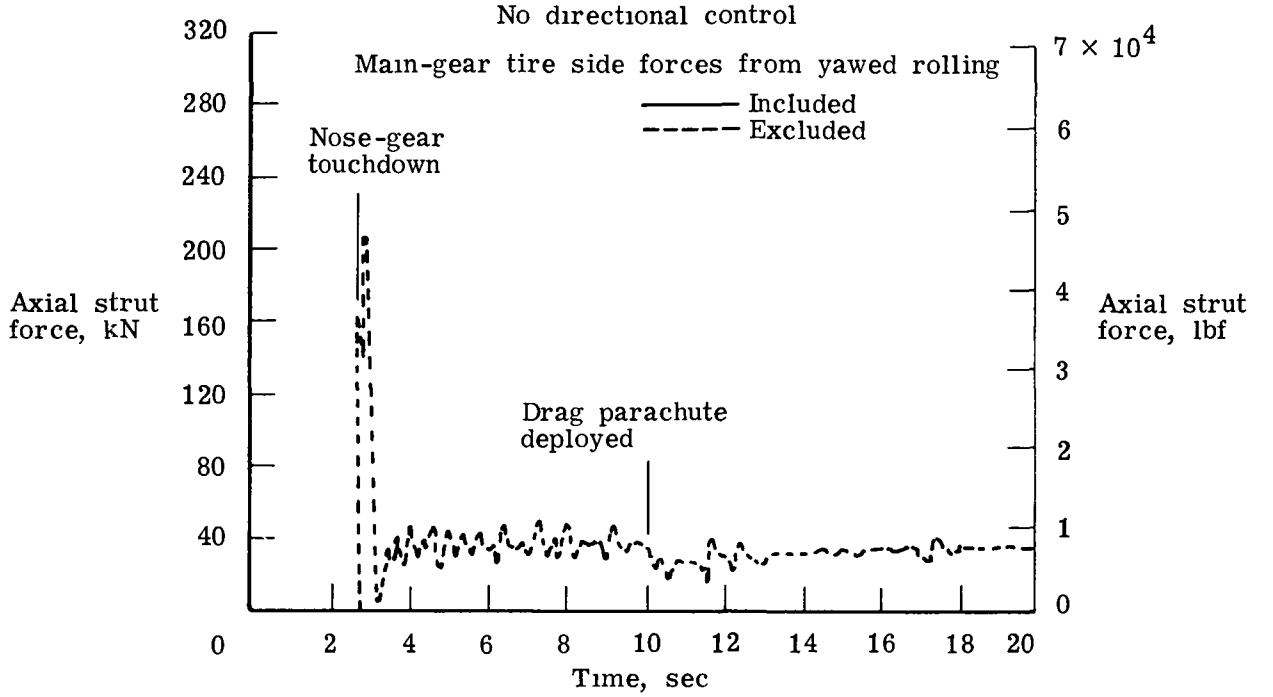

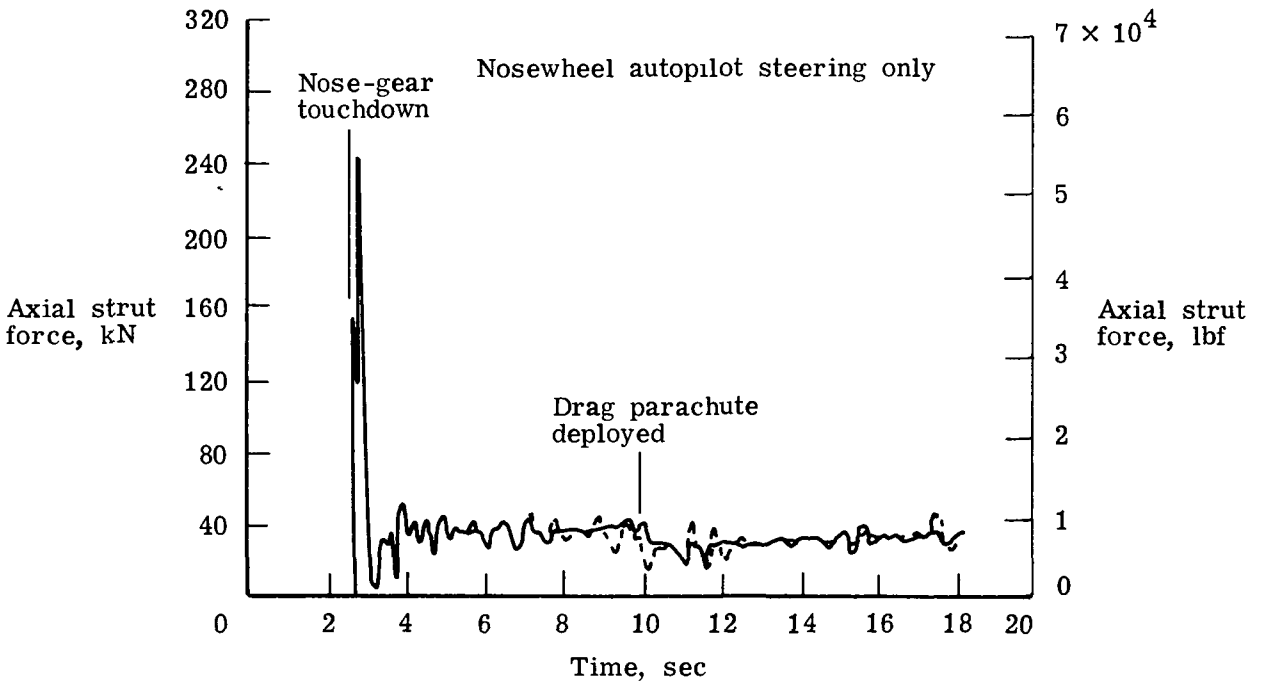

(l) Nose-gear axial strut force.

Figure 4.- Concluded.

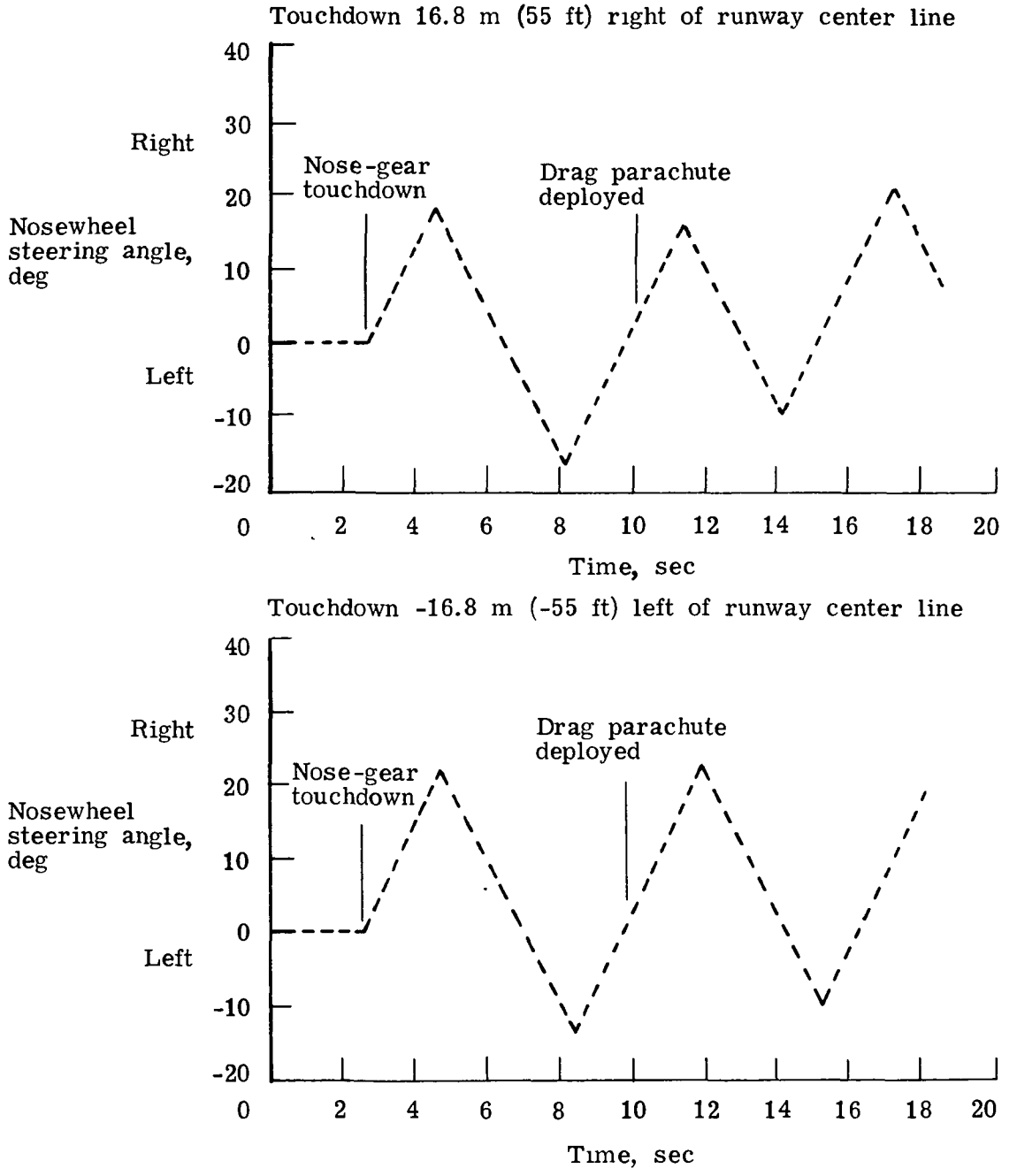

(a) Nosewheel steering angle.

Figure 5.- Analytical data for airplane crosswind landings with nosewheel autopilot steering only. Touchdowns ±16.8 m (±55 ft) right and left of runway center line. Wind velocity 7.62 m/sec (25 ft/sec) from the left. Main-gear tire side forces from yawed rolling excluded.

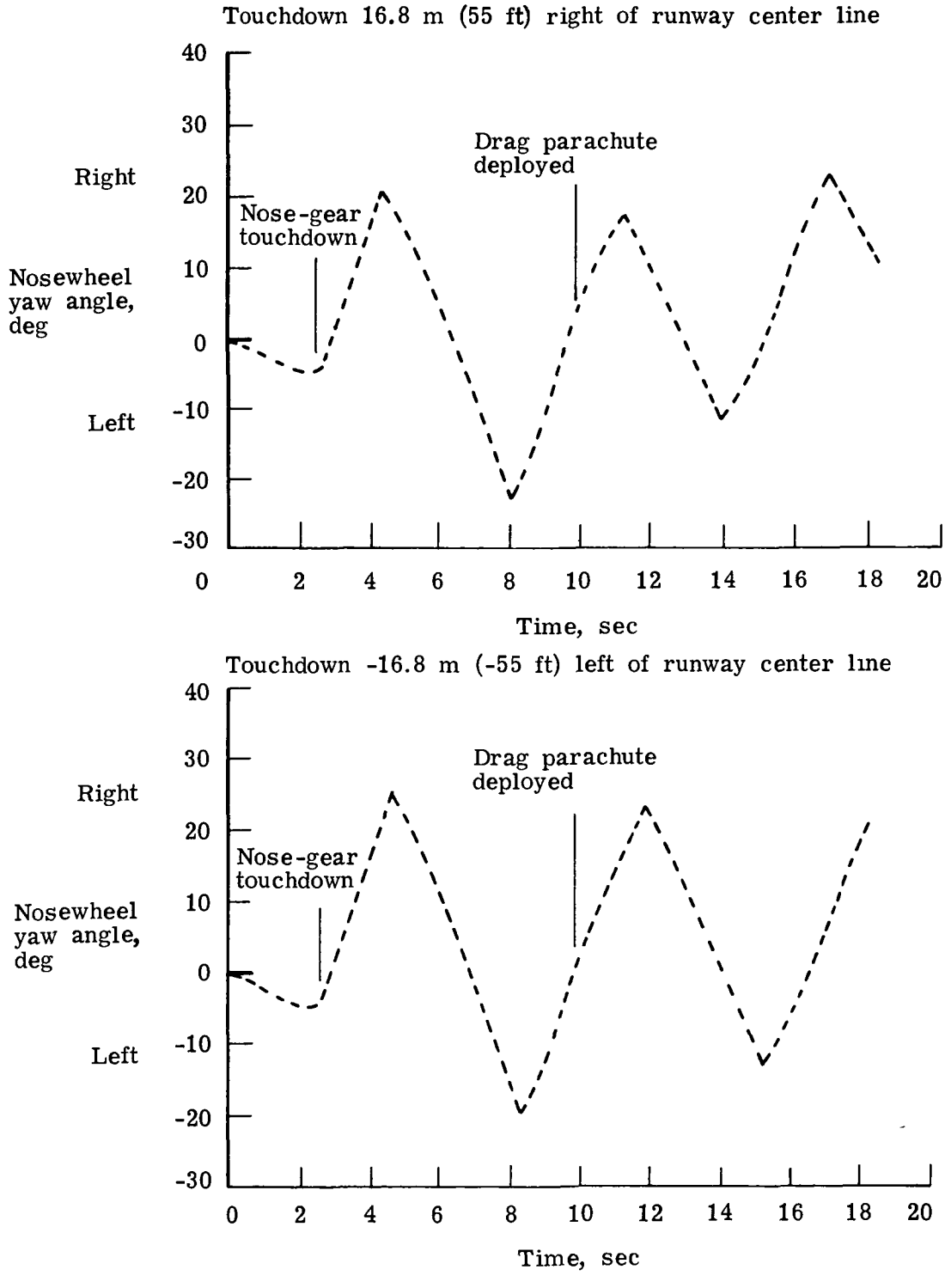

(b) Nosewheel yaw angle.

Figure 5.- Continued.

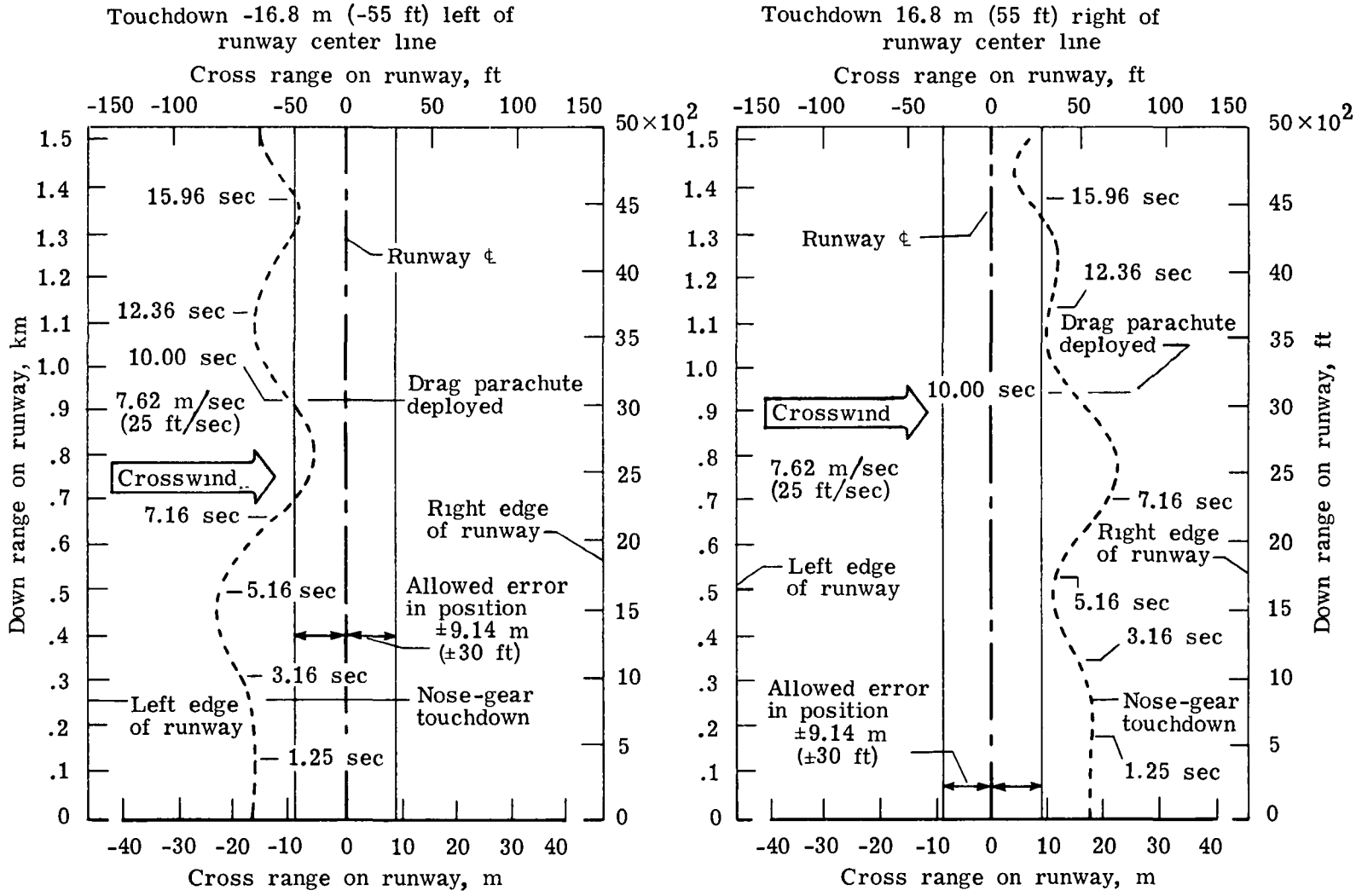

(c) Airplane c.g. position on runway.

Figure 5.- Concluded.

1 Report No	2 Government Accession No	3 Recipient's Catalog No
NASA TM-78768		

4 Title and Subtitle	5 Report Date
IMPROVEMENTS TO THE FATOLA COMPUTER PROGRAM INCLUDING NOSEWHEEL STEERING - SUPPLEMENTAL INSTRUCTION MANUAL	December 1978
	6 Performing Organization Code

7 Author(s)	8 Performing Organization Report No
Huey D. Carden and John R. McGehee	L-12295
	10 Work Unit No 517-53-13-14
9 Performing Organization Name and Address NASA Langley Research Center Hampton, VA 23665	11 Contract or Grant No
	13 Type of Report and Period Covered Technical Memorandum
12 Sponsoring Agency Name and Address National Aeronautics and Space Administration Washington, DC 20546	14 Sponsoring Agency Code

15 Supplementary Notes

16 Abstract

Modifications to a multi-degree-of-freedom flexible aircraft take-off and landing analysis (FATOLA) computer program, which improved its simulation capabilities, are discussed, and supplemental instructions for use of the program are included. Sample analytical results which illustrate the capabilities of an added nosewheel steering option indicate consistent behavior of the airplane tracking, attitude, motions, and loads for the landing cases and steering situations which were investigated.

17 Key Words (Suggested by Author(s))	18 Distribution Statement
Landing analysis Flexible aircraft Aircraft response Landing behavior	Unclassified - Unlimited Subject Category 05

19 Security Classif (of this report)	20 Security Classif (of this page)	21 No of Pages	22 Price*
Unclassified	Unclassified	61	$5.25

* For sale by the National Technical Information Service, Springfield, Virginia 22161

NASA-Langley, 1978

National Aeronautics and Space Administration

Washington, D.C.
20546

Official Business
Penalty for Private Use

THIRD-CLASS BULK RATE

Postage and Fees Paid
National Aeronautics and Space Administration
NASA-451

U.S.MAIL

5 2 1U,A, 120178 S90844HU
MCDONNELL DOUGLAS CORP
ATTN: PUBLICATIONS GROUP PR 15246-A
P O BOX 516
ST LOUIS MO 63166

NASA

POSTMASTER: If Undeliverable (Section 158 Postal Manual) Do Not Return